Phenomenology of an E_6 inspired extension of the Standard Model: Higgs sector

Sanchari Bhattacharyya[*] and Anindya Datta[†]

Department of Physics, University of Calcutta, 92, Acharya Prafulla Chandra Road, Kolkata 700009, India

We investigate a variant of the left-right symmetric model based on the $SU(3)_C \otimes SU(2)_L \otimes U(1)_L \otimes SU(2)_R \otimes U(1)_R$ gauge group (32121). Spontaneously breaking of 32121 down to the Standard Model (SM) gauge group requires a bidoublet under $SU(2)_L \otimes SU(2)_R$, a right-handed doublet scalar under $SU(2)_R$, along with a $SU(2)$ singlet scalar boson. Symmetry breaking leads to several neutral and charged massive gauge bosons apart from the SM W and Z. The Large Hadron Collider (LHC) results for the search of heavy gauge bosons can be used to constrain the vacuum expectation values responsible for giving masses to these extra heavy gauge bosons. The physical spectrum of the scalar bosons contains several neutral CP-even and CP-odd states and a couple of charged scalars apart from the SM-like Higgs boson. We have put constraints on the masses of some of these scalars from the existing LHC data. The possible decay rates and production cross sections of these scalars have been investigated in some detail. Production cross sections for some of the scalars look promising at the 14 and 27 TeV runs of the LHC with the high luminosity option. We keep, in our model, all the fermions present in the 27-dimensional fundamental representation of E_6. Mass limit of one such exotic lepton has also been derived from present LHC data. It is noted that some of these neutral exotic lepton or neutral scalar bosons of this model can serve the purpose of cold dark matter.

I. INTRODUCTION

The Standard Model (SM) of particle physics has been extremely successful in describing the interactions of elementary particles and fundamental forces operative in microscopic world. Probably the most subtle prediction of the SM has been the existence of a scalar boson, the Higgs boson, which is responsible for giving masses to all the elementary particles. With the discovery of Higgs boson [1,2] at the Large Hadron Collider (LHC), CERN, all the predictions of the SM has been tested. In spite of its immense success, the SM in its original form miserably fails to explain one important piece of experimental observations, namely, the existence of dark matter (DM), a new kind of very weakly interacting but massive matter pervading the whole Universe. Moreover, it is very crucial to know whether the discovered 125 GeV Higgs boson is the sole agent for electroweak symmetry breaking or a more

rich scalar sector is responsible for such an act. There are several theoretical studies [3] that have been devoted to investigate the phenomenology of extended Higgs sectors. It is important to note that any model with extended scalar sector must contain a physical CP-even scalar boson with exactly the same properties of the SM Higgs. The extended scalar sector may also be instrumental in resolving some of the shortcomings of the SM. As for example, extended Higgs sectors with singlet scalars may resolve the problem of dark matter [4]. Left-right (LR) symmetric triplet Higgs models are very popular in explaining neutrino masses via seesaw mechanisms [5,6]. Multi-Higgs doublet models have been used in explaining flavor problems [7]. An added bonus for many such models with an extended Higgs sector is a possibility of a stable neutral scalar that may act as a suitable candidate for DM. On the experimental front, signatures for extra neutral and charged scalar bosons have already been in the top of the agenda for all the past and present experimental programmes. Unfortunately, the evidence for the SM-like Higgs boson has been observed so far. Present precision of experimental data on Higgs signal strengths in different channels and our lack of experimental knowledge on Higgs trilinear coupling limits us from conclusively deciding whether the 125 GeV boson is the only agent of electroweak symmetry breaking [8]. In near future, with the high luminosity (HL) 14 (27) TeV run of

the LHC we expect these pictures to be more clearer. So it is of utmost priority for particle physics community to construct such models with extended scalar and/or gauge sector and check whether these models are consistent with the available and future experimental data from the LHC. A number of such models have been proposed and their possible experimental signatures at the LHC have been sought for. Unfortunately, many such efforts have been futile so far. Nonobservation of any signature of physics beyond the SM (whether supersymmetry [9] or extradimension [10]), only pushes the scale of such new dynamics in upward direction.

In an endeavor to construct a model that has a rich scalar sector satisfying the LHC data we turn our attention to an unifying gauge group E_6 [11], which can be broken down to $[SU(3)]^3$ followed by a further breakdown to $SU(3)_C \otimes SU(2)_L \otimes U(1)_L \otimes SU(2)_R \otimes U(1)_R$ (32121). We will not be interested in the dynamics that may be responsible for the aforementioned symmetry breaking chain, rather we will be investigating the appearance of the SM gauge group from 32121 and the resulting phenomenology of additional particles and their interactions among themselves or with the particles of SM. The main advantage of working in a framework of unifying group like E_6 is the natural appearance of right-handed neutrinos as well as three generations of heavy neutral leptons, singlet under either of $SU(2)$ groups. The right-handed heavy neutrinos may be responsible for neutrino mass generations via the (type-I) seesaw mechanism. This model contains a large number of neutral and charged scalar bosons after the spontaneous breakdown of $SU(2)_L \otimes U(1)_L \otimes SU(2)_R \otimes U(1)_R$ to the electroweak (EW) gauge group of the SM. These color singlet scalars originate from a $(\mathbf{1}, \mathbf{3}, \mathbf{\bar{3}})$ representation of $[SU(3)]^3$. The presence of such a rich scalar sector is one of the reasons behind the present investigation. Furthermore, several exotic fermions will arise from the 27-dimensional fundamental representation of E_6. Some of the neutral Higgs bosons and charge neutral leptons may also serve the purpose of dark matter. However, in this article we will mainly investigate the phenomenology of the extended scalar sector. A separate study will be devoted to the DM aspect of this model.

Although, the scalar sector of the model under consideration have many similarities with that of the left-right model, the phenomenology of the scalar sector has some distinct features that are different from the left-right symmetric model (LRSM). In the present work, we have banked on these features of the model to distinguish it from the often studied models like LRSM. Let us emphasize on the novelty of the present work in the following:

(i) Although the 32121 gauge group respects the LR symmetry, the model under consideration is different from the conventional LRSM. The first hint of this difference comes from the fact that both the bidoublet vacuum expectation values (VEVs) k_1 and k_2

cannot be simultaneously set to nonzero values unlike its more familiar variant based on $SU(2)_L \times SU(2)_R \times U(1)_{B-L}$ unless we consider a trilinear term in the scalar potential. Even after adding such a term that comes out to be small along with the small value of k_2, the phenomenology of this model remains practically the same as the $k_2 = 0$ case. This makes the phenomenology of the scalar sector of 32121 model different from LRSM.

(ii) We have considered the complete set of fermions arising from the **27**-dimensional representation of E_6. Some of these fermions are stable but have electric charges. We have for the first time derived bounds on their masses from the present LHC data. A detailed endeavor from our experimentalist friends to study their signature including detector simulation is presently unavailable and is urgently needed.

(iii) Although one of the charged Higgs bosons arising in the model has a conventional decay to tb, the other one is stable and produces a charged track in the detector. Such stable charged bosons are not present in the LRSM and their signatures have not been discussed in the present literature so far.

(iv) The pair production of charged and neutral Higgs bosons arising from left-handed doublet will produce either two charged tracks or a single charged track in the detector, giving rise to a background free novel signature of this model.

(v) Presence of a heavy neutral gauge boson, A' apart from Z' (arising because of the presence of $SU(2)_R$, can be identified with the Z_R in LRSM) is also a hall mark of the model under the consideration. This neutral boson arises due to the extra $U(1)$ factor in 32121 and couples to all the SM fermions, in contrast to several extensions of the SM by an extra $U(1)$, where this heavy neutral state has selective coupling with the SM fermions. Unlike the LRS model, where only one heavy neutral gauge boson is present, 32121 is characterized by two such states with similar properties but having different masses.

(vi) Three possible dark matter candidates in the forms of an exotic fermion and a scalar and a pseudoscalar originating from left doublet, are present in the spectrum. Although we will not discuss the direct detection bounds or relic density, a lower bound on the mass of the scalar has been derived indirectly from the LHC data in the present analysis.

Before we come to an end of this section, it is important to mention that we have only guided by the framework of E_6 to study the phenomenology of the a set of scalars whose masses are somehow interlaced due to the structure of the scalar potential respecting the local 32121 gauge symmetry. Similarly, the gauge group and complete set of a **27**-plet of fermions are chosen from a low energy point of view. Let us reemphasize that we will not study the

symmetry breaking chain $E_6 \rightarrow [SU(3)]^3 \rightarrow 32121$, neither we start with an unifying Yukawa texture appropriate for E_6 starting from the Grand Unified Theory (GUT) scale to generate the same at the EW scale by the renormalization group equation running. The Yukawa matrices in our analysis have been assumed to be nondiagonal. However, we will not discuss the pattern of masses and mixings for the exotic fermions present in the spectrum. The physical masses and mixings (in the case of the SM sector) have been assumed to be in consistency with the observed values of SM fermions while, for the exotic sector, they are free parameters defined at the EW scale. So, our connection to E_6 is only confined to the choice of gauge group and choice of fermions at low energy, without considering any effect from high scale physics creeping in due to renormalization.

Plan of the article is the following. In Sec. II, we discuss the symmetry breaking mechanism and spectra of Higgs bosons after spontaneous symmetry breaking (SSB). This section will also contain a discussion of gauge boson masses and fermion Yukawa interaction with the scalars. In the next section we will discuss in detail the phenomenology of the physical Higgs bosons which arise in the model after SSB. The decay branching ratios (BRs) and production cross sections of such Higgs bosons are presented in Sec. III in the context of the 14 and 27 TeV runs of the LHC. Finally, we conclude in Sec. IV.

II. THE DESCRIPTION OF THE $SU(3)_C \otimes SU(2)_L \otimes U(1)_L \otimes SU(2)_R \otimes U(1)_R$ MODEL

In this article, we will be interested in an extension of the SM whose root can be traced back to the grand unified group E_6. However at the energy scale of the LHC experiment in which we are interested, we keep all the fermions and Higgs multiplets excepting a few colored scalar bosons, which naturally arise in the 27-dimensional fundamental representation of E_6. However, to keep the number of matter fields in our model to a minimum, we will assume that the colored scalars are too heavy (of the order of symmetry breaking scale of $[SU(3)]^3$) to affect the phenomenology at the LHC energy.[1] Higgs multiplets will be instrumental in breaking down $SU(3)_C \otimes SU(2)_L \otimes U(1)_L \otimes SU(2)_R \otimes U(1)_R$ to the SM the gauge group, while the complete set of fermions present in the **27**-plet are necessary for anomaly cancellation. However, this choice of fermion representations used in our analysis is no way unique. One can have a vanishing anomaly contribution only by considering the left- and right-handed fermion doublets $L_L, L_R, Q_L,$ and Q_R. Hyper-charge assignments of

---

[1]If we intend to break the $[SU(3)]^3$ to 31221 by embedding the former into a five-dimensional manifold and applying appropriate orbifold boundary conditions, then one may get rid of such colored scalars by choosing appropriate boundary conditions on these fields at the orbifold boundaries [12].

TABLE I. Fermions and bosons in the 32121 model with their respective quantum numbers.

		3_C	2_L	2_R	1_L	1_R
Fermions	L_L	1	2	1	$-1/6$	$-1/3$
	$\bar{L}_R$	1	1	2	$1/3$	$1/6$
	$\bar{L}_B$	1	2	2	$-1/6$	$1/6$
	$\bar{L}_S$	1	1	1	$1/3$	$-1/3$
	Q_L	3	2	1	$1/6$	0
	$\bar{Q}_R$	$\bar{3}$	1	2	0	$-1/6$
	$\bar{Q}_{LS}$	$\bar{3}$	1	1	$-1/3$	0
	Q_{RS}	3	1	1	0	$1/3$
Bosons	Φ_B	1	2	2	$1/6$	$-1/6$
	Φ_L	1	2	1	$1/6$	$1/3$
	Φ_R	1	1	2	$-1/3$	$-1/6$
	Φ_S	1	1	1	$-1/3$	$1/3$
Gauge bosons	$G^i, i = 1, ..., 8$	8	1	1	0	0
	$W_L^i, i = 1, 2, 3$	1	3	1	0	0
	$W_R^i, i = 1, 2, 3$	1	1	3	0	0
	B_L	1	1	1	0	0
	B_R	1	1	1	0	0

the rest of the fermion multiplets listed in Table I can then be done by the consideration of anomaly cancellation among the exotic fermions and can be done in more than one way. We have presented two such cases in Table II. It is important to note that, in such a situation, $U(1)_{L,R}$ charges for the Higgs multiplets will be different from the case presented in this analysis. However, we will not consider such a situation and present our phenomenological analysis with a complete set of fermions arising from the **27**-plet.

TABLE II. Fermions and scalars in the 32121 model with their respective quantum numbers. The important thing to note here is that the $U(1)_L$ hypercharges of Q_{LS} and Q_{RS} have to be the same to cancel chiral anomaly. This is similar for the case of $U(1)_R$ too. But with $U(1)_L$ and $U(1)_R$, the hypercharges for each of them may not be equal. That depends upon the charge assignment of Q_{LS}, Q_{RS}. However, we consider that Q_{LS}, Q_{RS} have 2/3 charge. So it is an easy way to choose the $U(1)_L$ and $U(1)_R$ hypercharges of Q_{LS} as well as having Q_{RS} be equal, i.e., 1/3.

	3_C	2_L	2_R	1_L	1_R
L_L	1	2	1	1	$-3/2$
$\bar{L}_R$	1	1	2	-1	$3/2$
Q_L	3	2	1	$-1/3$	$1/2$
$\bar{Q}_R$	$\bar{3}$	1	2	$1/3$	$-1/2$
Φ_B	1	2	2	0	0
Φ_R	1	1	2	1	$-3/2$
Φ_S	1	1	1	0	0
$\bar{L}_B$	1	2	2	0	0
$\bar{Q}_{LS}$	$\bar{3}$	1	1	$1/3$	$1/3$
Q_{RS}	3	1	1	$-1/3$	$-1/3$
$\bar{L}_S$	1	1	1	0	0

Gauge bosons present in this model automatically follows from the gauge group of our interest. The matter and gauge fields that are present in our model are listed in Table I.[2]

The first block represents the minimal matter contents in the fermion sector, i.e., SM fermions with right-handed neutrinos. The scalars in the next block will provide us a gauge invariant Yukawa Lagrangian generating the masses of the SM fermions and Majorana mass for ν_R. We can generate the masses of all the exotic fermions with Φ_S.

The third block represents the other beyond the Standard Model (BSM) fermions present in **27**-plet and separately cancels chiral anomaly. L_B is a SU(2) doublet but an U(1) singlet, while L_S is a pure singlet. Here are two cases. For Q_{LS} as well as Q_{RS}, separately,

(1) If the $U(1)_L$ hypercharge is equal to the $U(1)_R$ hypercharge (i.e., same value/sign), then Q_{LS}, Q_{RS} will be vectorlike and they will not contribute in anomaly cancellation.

(2) If the $U(1)_L$ hypercharge is not equal to the $U(1)_R$ hypercharge (i.e., different value/sign), Q_{LS}, Q_{RS} will be chiral fermions and will contribute in anomaly cancellation.

A. Scalar sector of $SU(3)_C \otimes SU(2)_L \otimes U(1)_L \otimes SU(2)_R \otimes U(1)_R$ model

We now briefly discuss the Higgs multiplets responsible for symmetry breaking and their interactions in this model. The scalar sector of the 32121 model contains one Higgs bidoublet (Φ_B), one left-handed (Φ_L) and one right-handed (Φ_R) weak doublets, and a singlet Higgs boson (Φ_S) with nonzero $U(1)$ charges. These scalars arise from the $(\mathbf{1}, \mathbf{3}, \bar{\mathbf{3}})$ representation of $[SU(3)]^3$. For a complete symmetry breaking mechanism from $32121 \rightarrow SU(3)_C \otimes SU(2)_L \otimes U(1)_Y \rightarrow SU(3)_C \otimes U(1)_{EM}$, the alignments of Higgs bidoublet, right (left)-handed doublet and the singlet will be the following.

$$\Phi_B = \begin{pmatrix} \frac{1}{\sqrt{2}}(k_1 + h_1^0 + i\xi_1^0) & h_1^+ \\ h_2^- & \frac{1}{\sqrt{2}}(k_2 + h_2^0 + i\xi_2^0) \end{pmatrix},$$

$$\Phi_L = \begin{pmatrix} h_L^+ \\ \frac{1}{\sqrt{2}}(v_L + h_L^0 + i\xi_L^0) \end{pmatrix}, \qquad \Phi_R = \begin{pmatrix} \frac{1}{\sqrt{2}}(v_R + h_R^0 + i\xi_R^0) \\ h_R^- \end{pmatrix}, \qquad \Phi_S = \frac{1}{\sqrt{2}}(v_S + h_S^0 + i\xi_S^0). \qquad (1)$$

The Higgs potential, $\mathcal{V}$, which obeys symmetry of the gauge group, can be written as a sum of two parts $\mathcal{V}_1$ and $\mathcal{V}_2$, where

$$\begin{aligned} \mathcal{V}_1 = &-\mu_1^2 \text{Tr}(\Phi_B^\dagger \Phi_B) - \mu_3^2(\Phi_L^\dagger \Phi_L + \Phi_R^\dagger \Phi_R) - \mu_4^2 \Phi_S^\dagger \Phi_S + \lambda_1 \text{Tr}[(\Phi_B^\dagger \Phi_B)^2] + \lambda_3(\text{Tr}[\Phi_B^\dagger \tilde{\Phi}_B]\text{Tr}[\tilde{\Phi}_B^\dagger \Phi_B]) \\ &+ \alpha_1(\Phi_S^\dagger \Phi_S)^2 + \beta_1 \text{Tr}[\Phi_B^\dagger \Phi_B](\Phi_S^\dagger \Phi_S) + \gamma_1[(\Phi_L^\dagger \Phi_L) + (\Phi_R^\dagger \Phi_R)](\Phi_S^\dagger \Phi_S) \\ &+ \rho_1[(\Phi_L^\dagger \Phi_L)^2 + (\Phi_R^\dagger \Phi_R)^2] + \rho_3[(\Phi_L^\dagger \Phi_L)(\Phi_R^\dagger \Phi_R)] + c_1 \text{Tr}[\Phi_B^\dagger \Phi_B][(\Phi_L^\dagger \Phi_L) + (\Phi_R^\dagger \Phi_R)] \\ &+ c_3[(\Phi_L^\dagger \Phi_B \Phi_B^\dagger \Phi_L) + (\Phi_R^\dagger \Phi_B^\dagger \Phi_B \Phi_R)] + c_4[(\Phi_L^\dagger \tilde{\Phi}_B \tilde{\Phi}_B^\dagger \Phi_L) + (\Phi_R^\dagger \tilde{\Phi}_B^\dagger \tilde{\Phi}_B \Phi_R)] \end{aligned} \qquad (2)$$

and

$$\mathcal{V}_2 = \mu_{BS}\text{Tr}[\Phi_B^\dagger \tilde{\Phi}_B]\Phi_S^* + \text{H.c.} \qquad (3)$$

All the parameters in $\mathcal{V}$ are considered to be real excluding any possibility of *CP* violation via the Higgs sector. $\mathcal{V}$ has a symmetry under the $L \leftrightarrow R$ exchange. In the above, $\tilde{\Phi}_B \equiv \sigma_2 \Phi_B^* \sigma_2$.

We note that $\mathcal{V}_1$ has a symmetry corresponding to global phase transformations on the fields

$$\begin{aligned} \Phi_B \rightarrow e^{i\theta_B}\Phi_B; & \quad \Phi_L \rightarrow e^{i\theta_L}\Phi_L; \\ \Phi_R \rightarrow e^{i\theta_R}\Phi_R & \quad \text{and} \quad \Phi_S \rightarrow e^{i\theta_S}\Phi_S. \end{aligned} \qquad (4)$$

However, $\mathcal{V}_2$, which is proportional to μ_{BS}, breaks this global symmetry explicitly (for example see Ref. [13]) otherwise respecting the symmetries of 32121 gauge group. This results in the appearance of bilinear terms like $h_1^0 h_2^0$, $h_1^+ h_2^-$. However, with both k_1, $k_2 \neq 0$, such bilinear terms also could be generated from the term proportional to λ_3. Setting one of these VEVs to zero automatically prohibits the appearance of such bilinear terms in the scalar potential. In other words, setting both k_1 and k_2 to their nonzero values excluding $\mathcal{V}_2$, would break the global symmetry in Eq. (4) spontaneously, which results into undesirable extra massless scalar modes. One can of course have nonzero k_1 and k_2 simultaneously, however in such a case, a trilinear term proportional to μ_{BS} is necessary to break the global symmetry explicitly and thus avoid the appearance of extra Goldstone modes.

---

[2]Electric charge, Q, is defined through the relation $Q = T_{3L} + T_{3R} + Y_L/2 + Y_R/2$. L and R carry their usual meaning. These quantum numbers for each multiplet of 32121 model have been noted in the Table I.

The kinetic Lagrangian for scalars is

$$\mathcal{L}_\Phi = \mathrm{Tr}[(\mathcal{D}_\mu \Phi_B)^\dagger (\mathcal{D}^\mu \Phi_B)] + (\mathcal{D}_\mu \Phi_L)^\dagger (\mathcal{D}^\mu \Phi_L) + (\mathcal{D}_\mu \Phi_R)^\dagger (\mathcal{D}^\mu \Phi_R) + (\mathcal{D}_\mu \Phi_S)^\dagger (\mathcal{D}^\mu \Phi_S). \tag{5}$$

It is needless to mention that covariant derivatives acting on different Higgs multiplets are not the same and contain appropriate gauge bosons in them.

The minimization conditions we obtain are the following:

$$2\sqrt{2}\mu_{BS}k_2 v_S + k_1(2\lambda_1 k_1^2 + 2(\lambda_1 + 2\lambda_3)k_2^2 - 2\mu_1^2 + (c_1 + c_4)v_L^2 + (c_1 + c_3)v_R^2 + \beta_1 v_S^2) = 0, \tag{6}$$

$$2\sqrt{2}\mu_{BS}k_1 v_S + k_2(2\lambda_1 k_2^2 + 2(\lambda_1 + 2\lambda_3)k_1^2 - 2\mu_1^2 + (c_1 + c_3)v_L^2 + (c_1 + c_4)v_R^2 + \beta_1 v_S^2) = 0, \tag{7}$$

$$v_L[(c_1 + c_4)k_1^2 + (c_1 + c_3)k_2^2 - 2\mu_3^2 + 2\rho_1 v_L^2 + \rho_3 v_R^2 + \gamma_1 v_S^2] = 0, \tag{8}$$

$$v_R[(c_1 + c_3)k_1^2 + (c_1 + c_4)k_2^2 - 2\mu_3^2 + 2\rho_1 v_R^2 + \rho_3 v_L^2 + \gamma_1 v_S^2] = 0, \tag{9}$$

$$2\sqrt{2}k_1 k_2 \mu_{BS} + v_S(\beta_1(k_1^2 + k_2^2) - 2\mu_4^2 + \gamma_1(v_L^2 + v_R^2) + 2\alpha_1 v_S^2) = 0. \tag{10}$$

From Eqs. (6) and (7),

$$\mu_1^2 = \frac{1}{2k_1}(2\sqrt{2}\mu_{BS}k_2 v_S + k_1(2k_1^2\lambda_1 + 2(\lambda_1 + 2\lambda_3)k_2^2 + (c_1 + c_4)v_L^2 + (c_1 + c_3)v_R^2 + \beta_1 v_S^2)), \tag{11}$$

$$\mu_1^2 = \frac{1}{2k_2}(2\sqrt{2}\mu_{BS}k_1 v_S + k_2(2k_2^2\lambda_1 + 2(\lambda_1 + 2\lambda_3)k_1^2 + (c_1 + c_3)v_L^2 + (c_1 + c_4)v_R^2 + \beta_1 v_S^2)). \tag{12}$$

Using Eqs. (11) and (12) for $k_1, k_2 \neq 0$, we have

$$\mu_{BS} = \frac{1}{\sqrt{2}v_S}\frac{k_1 k_2}{k_2^2 - k_1^2}\left((c_3 - c_4)\frac{v_L^2 - v_R^2}{2} - 2\lambda_3(k_2^2 - k_1^2)\right). \tag{13}$$

Spontaneous breaking of left-right symmetry demands $v_R \neq 0$. Thus Eq. (9) results in

$$\mu_3^2 = \frac{1}{2}[(c_1 + c_3)k_1^2 + \rho_3 v_L^2 + 2\rho_1 v_R^2 + \gamma_1 v_S^2]. \tag{14}$$

The choice $v_L \neq 0$ leads to the appearance of an extra massless scalar mode that is undesirable.[3] So we stick to the case with $v_L = 0$.

To break the extra $U(1)$ we have to opt for $v_S \neq 0$ resulting in [from Eq. (10)]

$$\mu_4^2 = \frac{1}{2v_S}(2\sqrt{2}k_1 k_2 \mu_{BS} + v_S(\beta_1(k_1^2 + k_2^2) + \gamma_1(v_L^2 + v_R^2) + 2\alpha_1 v_S^2)). \tag{15}$$

Once we fix the minimization conditions of the Higgs potential, we are ready to note the Higgs mass matrices under such an alignment of the vacuum. However before delving into the details of scalar mass matrices let us make some brief comments on an important issue related to the minimum of the scalar potential. It is important to note that a scalar potential such as Eq. (2) depending on so many fields may have more than one minima having varying depths. Thus merely satisfying the minimization condition (by scalar potential parameters) does not ascertain that one is at the deepest minimum of the potential. In principle, different choices of the scalar potential parameters correspond to minima of different depths. Moreover, radiative corrections can significantly change the structure of the scalar potential and consequently change the depths of different minima of the potential. Hence, it is expected that one must at least incorporate one-loop corrections to the scalar potential to before looking for the deepest minima. However the exercise of calculating an effective potential at one loop for our model is beyond the scope of the present analysis. So we stick to the tree level potential and have not tried to look for its deepest minima. As long as the tunneling time from the false vacuum to the true (deepest) vacuum is larger than the lifetime of the Universe, sitting at a minimum other than the deepest one is not always hazardous. However a realistic estimation of this tunneling time also requires a one loop corrected effective

---

[3]This is related to the spontaneous breakdown of a global symmetry of the defined in Eq. (4).

potential of our model. A recent study [14] has been devoted to the analysis of the tree level scalar potential with particular emphasis on vacuum alignment and structure of minima of the potential. We would like to note that alignment of the vacuum used in our analysis satisfies the criterion of a good vacuum á la [14].

In the following, we note the CP-even, CP-odd, and charged scalar mass matrices after replacing μ_1, μ_{BS}, μ_3, and μ_4 using Eqs. (11), (13), (14), and (15), respectively.

In a basis, defined by the fields $\{h_1^0, h_2^0, h_L^0, h_R^0, h_S^0\}$, the square of CP-even mass matrix (M_r^{02}) is

$$
\begin{pmatrix}
2\lambda_1 k_1^2 + k_2^2 \Delta' & 2\lambda_1 k_1 k_2 + k_1 k_2 \Delta' & 0 & (c_1 + c_3)k_1 v_R & \beta_1 k_1 v_S - \frac{k_1 k_2^2 \Delta'}{v_S} \\
2\lambda_1 k_1 k_2 + k_1 k_2 \Delta' & 2\lambda_1 k_2^2 + k_1^2 \Delta' & 0 & (c_1 + c_4)k_2 v_R & \beta_1 k_2 v_S - \frac{k_1^2 k_2 \Delta'}{v_S} \\
0 & 0 & \frac{1}{2}((c_4 - c_3)k_-^2 + (\rho_3 - 2\rho_1)v_R^2) & 0 & 0 \\
(c_1 + c_3)k_1 v_R & (c_1 + c_4)k_2 v_R & 0 & 2\rho_1 v_R^2 & \gamma_1 v_R v_S \\
\beta_1 k_1 v_S - \frac{k_1 k_2^2 \Delta'}{v_S} & \beta_1 k_2 v_S - \frac{k_1^2 k_2 \Delta'}{v_S} & 0 & \gamma_1 v_R v_S & 2\alpha_1 v_S^2 + \frac{k_1^2 k_2^2 \Delta'}{v_S^2}
\end{pmatrix}, \quad (16)
$$

where $k_\pm^2 = k_1^2 \pm k_2^2$ and $\Delta' = \frac{(4\lambda_3 k_-^2 + (c_4 - c_3)v_R^2)}{2k_-^2}$.

While, the square of CP-odd mass matrix (M_i^{02}) in $\{\xi_1^0, \xi_2^0, \xi_L^0, \xi_R^0, \xi_S^0\}$ basis is

$$
\begin{pmatrix}
k_2^2 \Delta' & k_1 k_2 \Delta' & 0 & 0 & \frac{k_1 k_2^2 \Delta'}{v_S} \\
k_1 k_2 \Delta' & k_1^2 \Delta' & 0 & 0 & \frac{k_1^2 k_2 \Delta'}{v_S} \\
0 & 0 & \frac{1}{2}[(c_4 - c_3)(k_1^2 - k_2^2) + (\rho_3 - 2\rho_1)v_R^2] & 0 & 0 \\
0 & 0 & 0 & 0 & 0 \\
\frac{k_1 k_2^2 \Delta'}{v_S} & \frac{k_1^2 k_2 \Delta'}{v_S} & 0 & 0 & \frac{k_1^2 k_2^2 \Delta'}{v_S^2}
\end{pmatrix}. \quad (17)
$$

Once we diagonalize the above matrix, the three zero eigenvalues of CP-odd mass matrix corresponds to three Goldstone bosons responsible for giving masses to heavy neutral gauge bosons.

The square of the charged scalar mass matrix ($M^{\pm 2}$), in the basis $\{h_1^+, h_2^+, h_L^+, h_R^+\}$, is the following:

$$
\begin{pmatrix}
\frac{(c_4 - c_3)k_1^2 v_R^2}{2k_-^2} & \frac{(c_4 - c_3)k_1 k_2 v_R^2}{2k_-^2} & 0 & \frac{1}{2}(c_3 - c_4)k_1 v_R \\
\frac{(c_4 - c_3)k_1 k_2 v_R^2}{2k_-^2} & \frac{(c_4 - c_3)k_2^2 v_R^2}{2k_-^2} & 0 & \frac{1}{2}(c_3 - c_4)k_2 v_R \\
0 & 0 & \frac{1}{2}(\rho_3 - 2\rho_1)v_R^2 & 0 \\
\frac{1}{2}(c_3 - c_4)k_1 v_R & \frac{1}{2}(c_3 - c_4)k_2 v_R & 0 & \frac{1}{2}(c_4 - c_3)k_-^2
\end{pmatrix}. \quad (18)
$$

Diagonalization of the above matrix gives us two massive charged scalars and two massless Goldstones corresponding to a couple of heavy charged gauge bosons.

We note that, with nonzero k_1 and k_2, W (and Z) masses get a contribution proportional to $(k_1^2 + k_2^2)^{\frac{1}{2}}$ while $W_L - W_R$ mixing is proportional to $\frac{k_1 k_2}{v_R^2}$ [see Eq. (27)]. The experimental limit on the $W_L - W_R$ mixing [15] forces one

to choose any one of these VEVs to be very small[4] compared to other keeping $(k_1^2 + k_2^2)^{\frac{1}{2}}$ fixed at 246 GeV. One can then safely assume that $k_1^2 + k_2^2 \approx k_1^2 - k_2^2 \approx k_1^2$.

---

[4]For example, if we set the mixing angle of $W_L - W_R$ at its maximum allowed value, then k_2 will be of the order of 0.27 GeV, assuming $k_1 > k_2$.

Thus in a small k_2 limit, we can rewrite the scalar mass matrices as

$$
M_r^{02} = \begin{pmatrix}
2\lambda_1 k_1^2 & 0 & 0 & (c_1+c_3)k_1 v_R & \beta_1 k_1 v_S \\
0 & \frac{1}{2}[4\lambda_3 k_1^2 + (c_4-c_3)v_R^2] & 0 & 0 & 0 \\
0 & 0 & \frac{1}{2}[(c_4-c_3)k_1^2 + (\rho_3-2\rho_1)v_R^2] & 0 & 0 \\
(c_1+c_3)k_1 v_R & 0 & 0 & 2\rho_1 v_R^2 & \gamma_1 v_R v_S \\
\beta_1 k_1 v_S & 0 & 0 & \gamma_1 v_R v_S & 2\alpha_1 v_S^2
\end{pmatrix}, \quad (19)
$$

$$
M_i^{02} = \begin{pmatrix}
0 & 0 & 0 & 0 & 0 \\
0 & \frac{1}{2}[4\lambda_3 k_1^2 + (c_4-c_3)v_R^2] & 0 & 0 & 0 \\
0 & 0 & \frac{1}{2}[(c_4-c_3)k_1^2 + (\rho_3-2\rho_1)v_R^2] & 0 & 0 \\
0 & 0 & 0 & 0 & 0 \\
0 & 0 & 0 & 0 & 0
\end{pmatrix}, \quad (20)
$$

$$
M^{\pm 2} = \begin{pmatrix}
\frac{1}{2}(c_4-c_3)v_R^2 & 0 & 0 & \frac{1}{2}(c_3-c_4)k_1 v_R \\
0 & 0 & 0 & 0 \\
0 & 0 & \frac{1}{2}(\rho_3-2\rho_1)v_R^2 & 0 \\
\frac{1}{2}(c_3-c_4)k_1 v_R & 0 & 0 & \frac{1}{2}(c_4-c_3)k_1^2
\end{pmatrix}. \quad (21)
$$

It is also evident that, in spite of setting $k_2 = 0$ and as a consequence $\mu_{BS} = 0$, the elements of scalar mass matrices, mass eigenvalues, and mixing matrices practically remains the same as before. It is easy to verify that in the limit $v_R, v_S \gg k_1 \gg k_2$ (the first inequality arises from the experimental lower limits on heavy gauge boson masses, discussed in a following section), the mass matrix defined in Eq. (16) will practically produce the same eigenvalues and mixing among the scalars as has been resulted from Eq. (19). Similarly Eqs. (17) and (18) will generate same masses and mixings as Eqs. (20) and (21) will do, respectively.

As mentioned above, the masses and mixings among the scalars in the $k_2 \neq 0, \mu_{BS} \neq 0$ case are nearly the same as the $k_2 = 0$ case, Although a nonzero k_2 would result into some new couplings among the scalars that are not present in the later case. Some new decay channels will open up for the scalars like h_2^0 and H_S^0. However, these new decay modes will not affect the decay patterns of the physical scalars in a significant way as the decay rates will be proportional to k_2^2. We will not discuss them any further. All the following analysis will be done in the $k_2 = 0$ limit, which could be viewed as some special but not phenomenologically different from the more general situation with both k_1 and k_2 set to nonzero values.

The scalar potential has 10 real parameters, $\lambda_1, \lambda_3, \rho_1, \rho_3,$ $c_1, c_3, c_4, \alpha_1, \beta_1,$ and γ_1. In order to find a set of acceptable values of the physical Higgs boson masses and the potential to be stable at least at classical level, the parameters of scalar potential must obey the following conditions:

$$
\lambda_1, (\lambda_1 + 2\lambda_3), \rho_1, \rho_3, (c_1+c_3), (c_1+c_4), \alpha_1, \beta_1, \quad \gamma_1 > 0. \quad (22)
$$

The condition that the physical charged Higgs mass squares be positive demands

$$
c_4 - c_3 > 0 \quad \text{and} \quad \rho_3 - 2\rho_1 > 0.
$$

Values of $(c_4 - c_3)$ and $(\rho_3 - 2\rho_1)$ can be constrained from a model independent experimental limit of a charged Higgs boson mass.

From the CP-even scalar mass matrix we notice that it is effectively a 3×3 mass matrix in $\{h_1^0, h_R^0, h_S^0\}$ basis and thus difficult to diagonalize analytically. However, one linear combination of $h_1^0, h_R^0,$ and h_S^0 will be definitely like the SM Higgs boson with mass 125 GeV and having similar properties with this:

$$
M_{r3\times3}^{02} = \begin{pmatrix}
2\lambda_1 k_1^2 & (c_1+c_3)k_1 v_R & \beta_1 k_1 v_S \\
(c_1+c_3)k_1 v_R & 2\rho_1 v_R^2 & \gamma_1 v_R v_S \\
\beta_1 k_1 v_S & \gamma_1 v_R v_S & 2\alpha_1 v_S^2
\end{pmatrix}. \quad (23)
$$

We will denote the eigenstates of mass matrix [Eq. (23)] by h^0, H_R^0, H_S^0. The rest of the two massive CP-even and two massive CP-odd scalars do not mix with others, and we shall use the same notation to identify the mass eigenstates as we have used to define gauge eigenstates. For the
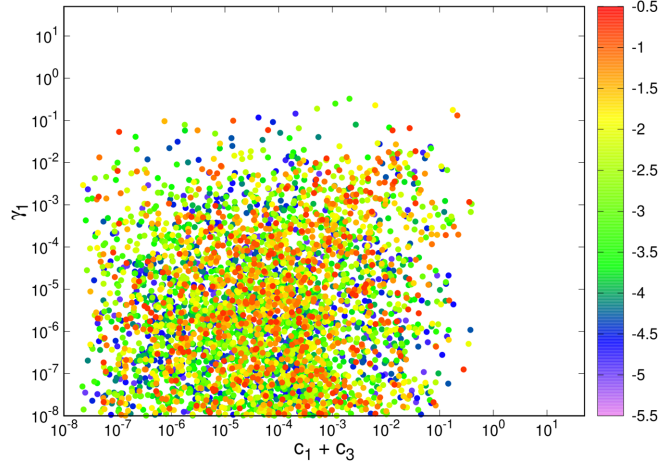
FIG. 1. Allowed parameter space for $(c_1 + c_3)$ and γ_1 for some fixed values of β_1. The side bar represents the values of β_1 in $\log_{10}$ scale.

charged Higgs sector, the two massive eigenstates will be denoted by $H_1^\pm$ (which is a linear combinations of $h_1^\pm$ and $h_R^\pm$) and $H_L^\pm$.

The 3×3 block of neutral CP-even mass matrix [see mass matrix (23)], can be diagonalized numerically. We must keep in mind that one of the eigenstates must correspond to the SM-like Higgs boson h^0. This implies that the mass eigenvalue and the corresponding eigenvector must be consistent with the measured value of SM Higgs boson mass and its signal strengths to different decay channels at the LHC. We have done a scan over the parameters of the mass matrix [Eq. (23)] over a range keeping the values of k_1, v_R, and v_S fixed. We will see in the next section that the value of k_1 is fixed from the W-boson mass, while a lower limit on the values of v_R and v_S can be obtained from the consideration of the masses of heavy gauge bosons W_R and A' arising in this model. While scanning over the parameters we have set the values of v_R and v_S at their lower limits of 14.7 and 13 TeV, respectively.

The result of the scan is presented in Fig. 1. For the points in the plot, value of one of the eigenstates satisfies the SM Higgs mass condition and Higgs signal strength to $b\bar{b}$ decay mode [15]. It can be seen from the plot that relatively larger values of the parameters controlling the off-diagonal terms of the mass matrix are possible. This in turn implies that the eigenstates (particularly the one which can be identified with h^0) are linear combinations of all three gauge states $\{h_1^0, h_R^0, h_S^0\}$; while performing this scan over a large range of parameter space, we have observed that in most cases it keeps λ_1 more or less fixed close to the value $\frac{m_{h^0}^2}{2k_1^2}$. But the values of ρ_1 and α_1 are completely unconstrained. Instead of diagonalizing the mass matrix numerically we have restricted ourselves to the values of $c_1 + c_3$ and γ_1 such that the corresponding off-diagonal

terms in the mass matrix can be neglected with respect to the diagonal terms. In this limit, large values of β_1 forces one to accept large values of α_1 so that SM Higgs signal strengths as calculated from the model is in agreement with experimental observation. Furthermore, we keep a tiny value for β_1 consistent with the above scan result. Under such assumptions about the values of these parameters, mass (squared) eigenvalues can be approximated by the following expressions:

$$
\begin{aligned}
m_{h^0}^2 &= \lambda_1 k_1^2 + \alpha_1 v_S^2 - \sqrt{\Delta}, \\
m_{H_R^0}^2 &\simeq 2\rho_1 v_R^2, \\
m_{H_S^0}^2 &= \lambda_1 k_1^2 + \alpha_1 v_S^2 + \sqrt{\Delta},
\end{aligned} \tag{24}
$$

with the eigenstate corresponding to the eigenvalue $m_{h^0}^2$ being identified with the SM-like Higgs boson with a mass of 125 GeV. Here $\Delta = (\alpha_1 v_S^2 - \lambda_1 k_1^2)^2 + \beta_1^2 k_1^2 v_S^2$. The mixing angle θ (operative between h^0 and H_S^0) in small β_1 limits can be written as

$$
\tan(2\theta) = \frac{\beta_1 k_1 v_S}{\alpha_1 v_S^2 - \lambda_1 k_1^2}. \tag{25}
$$

We will be mainly interested in a study considering in the above-mentioned simplified version of the parameter space where we have only considered that H_S^0 has a tiny mixing (proportional to β_1) with the SM-like Higgs boson h^0. At the end, we will make a comment about the possible outcome of a study with non-negligible values of $c_1 + c_3$ and γ_1.

B. Gauge sector of the $SU(3)_C \otimes SU(2)_L \otimes U(1)_L \otimes SU(2)_R \otimes U(1)_R$ model

The gauge sector of the 32121 model consists of 16 gauge bosons, namely the eight gluons ($G^{a'}, a' = 1, \ldots, 8$), $SU(2)_{L,R}$ gauge bosons, $W_L^a, W_R^a, (a = 1, 2, 3)$, and two $U(1)$ gauge bosons B_L and B_R. Their interactions are governed by five gauge coupling constants $g_3, g_{2L}, g_{2R}, g_{1L}$, and g_{1R}.

The gauge kinetic Lagrangian can be expressed in terms of a field strength tensor in the usual way,

$$
\begin{aligned}
\mathcal{L}_{GK} = &-\frac{1}{4} G^{a' \mu\nu} G_{\mu\nu}^{a'} - \frac{1}{4} W_L^{a\mu\nu} W_{L\mu\nu}^a - \frac{1}{4} W_R^{a\mu\nu} W_{R\mu\nu}^a \\
&- \frac{1}{4} B_L^{\mu\nu} B_{L\mu\nu} - \frac{1}{4} B_R^{\mu\nu} B_{R\mu\nu} - \frac{\epsilon}{2} B_L^{\mu\nu} B_{R\mu\nu}.
\end{aligned} \tag{26}
$$

The last term in Eq. (26) represents the $U(1)_{L,R}$ kinetic mixing proportional to a dimensionless parameter ϵ. A nonzero value of the kinetic mixing coefficient ϵ would modify the extra heavy neutral gauge boson coupling to a pair of fermions [16]. However, the focus of our present

study is not in that direction and we will use $\epsilon = 0$ in our following analysis.

The charged gauge bosons mass matrix (in the $W_L - W_R$ basis) follows from the Higgs kinetic Lagrangian [Eq. (5)] in the k_1, $k_2 \neq 0$ limit:

$$M^2_{W^\pm} = \frac{1}{4}\begin{pmatrix} g^2_{2L}(k_1^2 + k_2^2) & -2g_{2L}g_{2R}k_1k_2 \\ -2g_{2L}g_{2R}k_1k_2 & g^2_{2R}(k_1^2 + k_2^2 + v_R^2) \end{pmatrix}, \quad (27)$$

which in a small k_2 limit appears as

$$M^2_{W^\pm} = \frac{1}{4}\begin{pmatrix} g^2_{2L}k_1^2 & 0 \\ 0 & g^2_{2R}(k_1^2 + v_R^2) \end{pmatrix}. \quad (28)$$

$$\frac{1}{2}\begin{pmatrix} \frac{1}{2}g^2_{2L}k_+^2 & -\frac{1}{2}g_{2L}g_{2R}k_+^2 & \frac{1}{6}g_{1L}g_{2L}k_-^2 & -\frac{1}{6}g_{1R}g_{2L}k_-^2 \\ -\frac{1}{2}g_{2L}g_{2R}k_+^2 & \frac{1}{2}g^2_{2R}(k_+^2 + v_R^2) & -\frac{1}{3}g_{1L}g_{2R}(\frac{1}{2}k_-^2 + v_R^2) & \frac{1}{6}g_{1R}g_{2R}(k_-^2 - v_R^2) \\ \frac{1}{6}g_{1L}g_{2L}k_-^2 & -\frac{1}{3}g_{1L}g_{2R}(\frac{1}{2}k_-^2 + v_R^2) & g^2_{1L}(\frac{1}{18}k_+^2 + \frac{2}{9}v_R^2 + \frac{2}{9}v_S^2) & g_{1L}g_{1R}(-\frac{1}{18}k_+^2 + \frac{1}{9}v_R^2 - \frac{2}{9}v_S^2) \\ -\frac{1}{6}g_{1R}g_{2L}k_-^2 & \frac{1}{6}g_{1R}g_{2R}(k_-^2 - v_R^2) & g_{1L}g_{1R}(-\frac{1}{18}k_+^2 + \frac{1}{9}v_R^2 - \frac{2}{9}v_S^2) & g^2_{1R}(\frac{1}{18}k_+^2 + \frac{1}{18}v_R^2 + \frac{2}{9}v_S^2) \end{pmatrix}, \quad (29)$$

which in small k_2 scenario practically becomes

$$M^2_{NG} = \frac{1}{2}\begin{pmatrix} \frac{1}{2}g^2_{2L}k_1^2 & -\frac{1}{2}g_{2L}g_{2R}k_1^2 & \frac{1}{6}g_{1L}g_{2L}k_1^2 & -\frac{1}{6}g_{1R}g_{2L}k_1^2 \\ -\frac{1}{2}g_{2L}g_{2R}k_1^2 & \frac{1}{2}g^2_{2R}(k_1^2 + v_R^2) & -\frac{1}{3}g_{1L}g_{2R}(\frac{1}{2}k_1^2 + v_R^2) & \frac{1}{6}g_{1R}g_{2R}(k_1^2 - v_R^2) \\ \frac{1}{6}g_{1L}g_{2L}k_1^2 & -\frac{1}{3}g_{1L}g_{2R}(\frac{1}{2}k_1^2 + v_R^2) & g^2_{1L}(\frac{1}{18}k_1^2 + \frac{2}{9}v_R^2 + \frac{2}{9}v_S^2) & g_{1L}g_{1R}(-\frac{1}{18}k_1^2 + \frac{1}{9}v_R^2 - \frac{2}{9}v_S^2) \\ -\frac{1}{6}g_{1R}g_{2L}k_1^2 & \frac{1}{6}g_{1R}g_{2R}(k_1^2 - v_R^2) & g_{1L}g_{1R}(-\frac{1}{18}k_1^2 + \frac{1}{9}v_R^2 - \frac{2}{9}v_S^2) & g^2_{1R}(\frac{1}{18}k_1^2 + \frac{1}{18}v_R^2 + \frac{2}{9}v_S^2) \end{pmatrix}. \quad (30)$$

In practical, the presence of this small k_2 will not sensitively affect the masses and mixings in the neutral gauge sector.

Before we make predictions about the masses of the neutral gauge bosons, let us make further assumption about the four gauge coupling constants. We will identify the $SU(2)_L$ of 32121 with the weak isospin group of the Standard Model. It follows automatically that $U(1)_Y$ of the SM will arise due to breaking of $SU(2)_R \otimes U(1)_L \otimes U(1)_R$. Consequently, one can identify g_Y [the $U(1)_Y$ gauge coupling constant with $g_Y = e/\cos\theta_W$] of the SM via the following relation:

$$\frac{1}{g_Y^2} = \frac{1}{g_{2R}^2} + \frac{1}{g_{1L}^2} + \frac{1}{g_{1R}^2}. \quad (31)$$

The above relation among the gauge couplings allows us to choose any two of g_{2R}, g_{1L}, and g_{1R} independently. In order to keep our Lagrangian manifestly LR symmetric, we assume $g_{2L} = g_{2R}$ and $g_{1L} = g_{1R}$. All our analysis presented in the following will be based on this assumption.

Eigenvalues of the already diagonalized mass matrix provide W_L and W_R masses. The experimentally measured value of W_L mass fixes k_1 at 246 GeV, if we set at $g_{2L} = e/\sin\theta_W$ where θ_W is the Weinberg angle. Throughout our article, we shall denote W_L as the SM W boson with a mass of 80.379 GeV [15]. Experimentally measured value of W mass would fix the value of k_1 and an experimental lower limit on W_R mass [17] provides a lower bound on $v_R (>14.7 \text{ TeV})$.

One can similarly obtain the mass matrix for neutral gauge bosons in the W_{3L}, W_{3R}, B_L, B_R basis, with $k_2 \neq 0$, M^2_{NG}:

To completely determine the gauge boson masses we need to know the values of the gauge coupling constants and three nonzero VEVs. The gauge coupling constants have been already fixed from the symmetry breaking condition and demand of manifest left-right symmetry. The value or allowed range of values of v_S remains to be known for evaluation of the gauge boson masses from Eqs. (28), (30). It is to be noted that v_S plays a crucial role in breaking $U(1)_L \otimes U(1)_R$. The tree level relation among m_Z, m_W, and $\cos\theta_W$ has been ensured by identifying the massless eigenstate (of M^2_{NG}) with the photon, which has equal coupling to left- and right-chiral fermions.

We have implemented the model Lagrangian in SARAH [18] as well as in FEYNRULES [19]. In the following analysis all the cross sections will be calculated with help of MADGRAPH5(v2.6.6) [20] using NNPDF23NLO parton distribution functions [21] with the factorization scale set equal to the average mass of the final state particles.

Upon diagonalization, one of the eigenvalues of Eq. (30) will give a zero eigenvalue corresponding to the photon. Another eigenvalue comes out to be nearly equal to 91.2 GeV, which we identify with the Z boson. Other
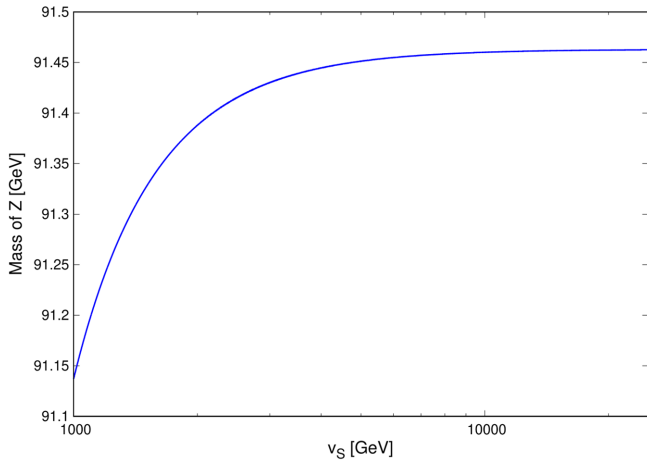
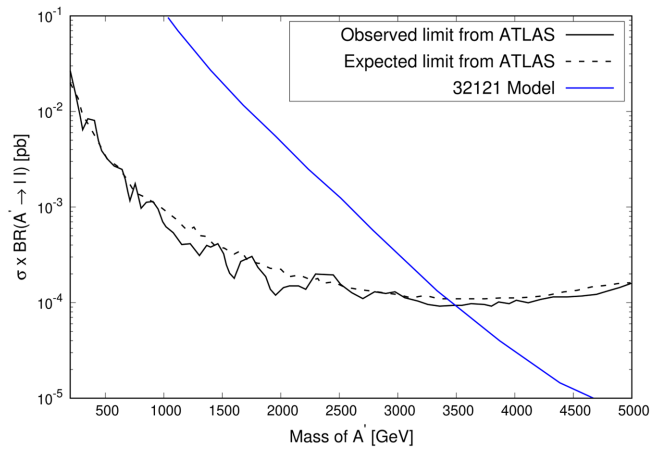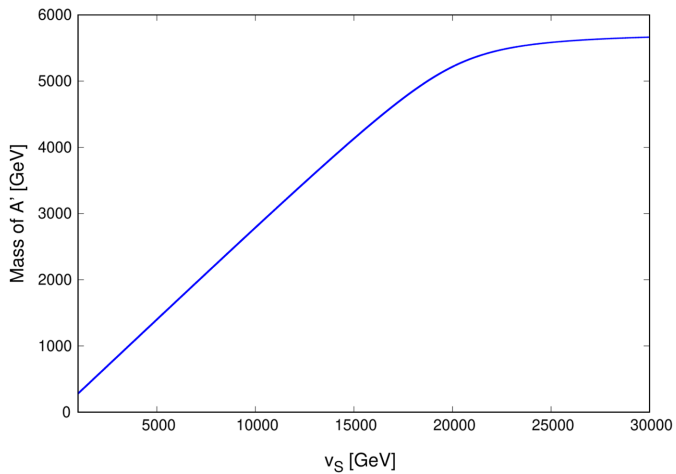FIG. 2.   Weak dependence of Z mass on v_S.

FIG. 4.   Production cross section, a $\sigma \times BR$ plot for a heavy neutral gauge boson production at the LHC. The black solid (dashed) line represents the observed (expected) 95% CL upper limit on $\sigma \times BR$ from ATLAS (with $\sqrt{s} = 13$ TeV, 36.1 fb^{-1}) considering dilepton decay channel of the produced gauge boson and the blue line corresponds to the prediction of 32121 model.

two eigenvalues correspond to two heavy neutral gauge bosons that we identify as Z' and A', the last one being a hall mark of an extra $U(1)$ gauge symmetry.

Figure 2 shows the weak dependence of Z mass on v_S, whereas Fig. 3 reveals a strong correlation between the mass of A' with v_S. Taking a hint from this fact, we would like to find an allowed range of v_S from the LHC data itself. In such an effort, an experimental search of a heavy neutral gauge boson at the LHC and its subsequent decay to a pair of leptons would be helpful. ATLAS collaboration at the LHC [22] has looked for a pair of high p_T leptons (e and μ) to put an upper limit on the production cross section times the branching ratio of a heavy neutral gauge boson at 13 TeV. We have translated this upper limit on the $\sigma \times BR$ to the mass of A'. In our model A' couples to both quarks and leptons with couplings proportional to their $U(1)_{L,R}$ charges. We present the $\sigma \times BR$ of A' in Fig. 4. The black solid and dashed lines represent the observed and expected 95% confidence level (CL) upper limit on the cross section

times branching ratio by ATLAS, respectively. While the blue solid line gives the $\sigma \times BR$ of A' in 32121 model as a function of A' mass. One can find a lower limit on A' mass equals to 3.5 TeV.

Knowledge of a lower limit on A' mass enables one to get a lower limit on v_S. $m_{A'}$ is a function of the gauge coupling constants and three nonzero VEVs necessary for symmetry breaking. The mass of A' has a very weak dependence on k_1 and v_R in comparison to v_S. Values of the gauge couplings and k_1 are fixed. And we set the value of v_R at its lower limit while obtaining a lower limit on v_S. We thus arrive at a lower limit on v_S, which equals to 12.61 TeV. $m_{A'}$ is a slowly increasing function of v_R. So one cannot arrive at an absolute lower limit on v_S. The allowed region of $v_R - v_S$ space has been presented in Fig. 5.
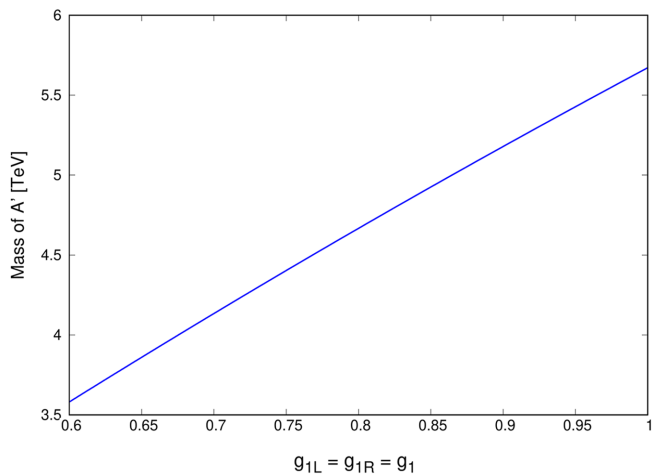

FIG. 3.   Dependence of A' mass on v_S (left panel) and on g_{1L} and g_{1R}, with $g_{1L} = g_{1R}$ for a fixed v_S (right panel).
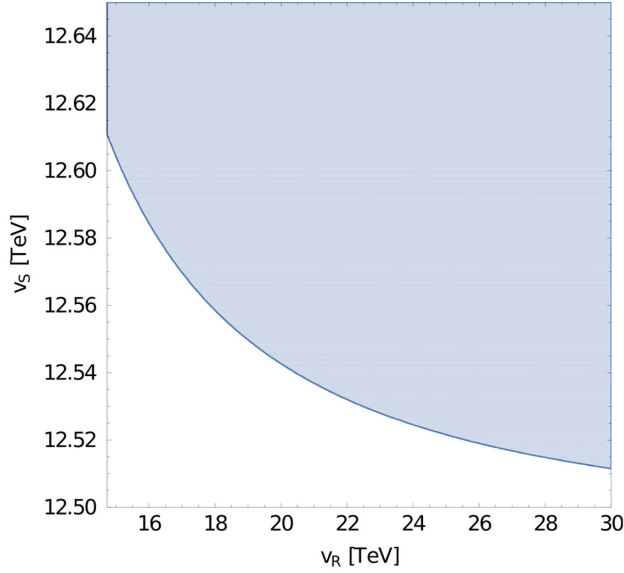
FIG. 5. Allowed region in $v_R - v_S$ space, obtained from the limits on A' mass. $m_{A'}$ has a strong dependence on v_S and has a milder dependence on v_R.

Z' mass on the other hand, is mainly controlled by v_R and it has a weak dependence on v_S. With v_R at its lower limit, Z' mass comes out to be 5.9 TeV. For such a massive Z', the cross section times its branching ratio to a pair of leptons is of the order of 10^{-3} fb. This rate is well below the upper limit of cross section times BR for a heavy neutral gauge boson by the ATLAS collaboration [22] and is presented in Fig. 4.

C. Fermion sector of the $SU(3)_C \otimes SU(2)_L \otimes U(1)_L \otimes SU(2)_R \otimes U(1)_R$ model

The gauge quantum numbers of the fermions have been already listed in Table I. In the following we note the fermions with their chiral components.

$$L_L = \begin{pmatrix} \nu_L \\ e_L \end{pmatrix}, \qquad L_R = \begin{pmatrix} \nu_R \\ e_R \end{pmatrix},$$

$$Q_L = \begin{pmatrix} u_L \\ d_L \end{pmatrix}, \qquad Q_R = \begin{pmatrix} u_R \\ d_R \end{pmatrix},$$

$$Q_{LS} = q_{SL}, \qquad Q_{RS} = q_{SR}, \qquad L_S = l_S, \quad \text{and}$$

$$L_B = \begin{pmatrix} N_1 & E_1 \\ E_2 & N_2 \end{pmatrix} \quad \text{with} \quad \bar{L}_B = \begin{pmatrix} \bar{N}_1 & \bar{E}_2 \\ \bar{E}_1 & \bar{N}_2 \end{pmatrix}. \tag{32}$$

Here, L_L, L_R, Q_L, Q_R represent SM fermions along with a right-handed neutrino (ν_R). Q_{LS} and Q_{RS} are color triplets and $SU(2)$ gauge singlet exotic quarks having $U(1)_L$ and $U(1)_R$ hypercharges, respectively. They together form a four-component Dirac spinor q_S. N_1 and N_2 are neutral heavy leptons while E_1 and E_2 are singly charged heavy leptons. They pairwise form four-component Dirac spinors,

N and E, respectively. l_S is a neutral exotic singlet fermion but carrying $U(1)_L$ and $U(1)_R$ gauge quantum numbers.

The fermionic sector of this model consists of several heavy leptons and quarks apart from theirs SM counterparts. We would like to spend few words on them. The presence of ν_R facilitates us to write a Dirac or Majorana mass for the neutrinos [6,23].[5] Heavy charged lepton $E^\pm$ and heavy neutrino N arise from the $SU(2)$ bidoublet L_B. These will couple to the SM gauge bosons and thus can be produced at the LHC. Similarly, $SU(2)$ singlet quarks Q_{LS} and Q_{RS} form a heavy quark of electric charge $+\frac{1}{3}$ of Dirac type. Finally, there remains a $SU(2)_{L,R}$ singlet lepton of zero electric charge. This could well be a candidate for dark matter. The assignment of $U(1)$ charges for the fermions, from the requirement of anomaly cancellation, is such that the exotic fermions can only couple to the gauge bosons but do not have any mixing with the SM fermions. This feature will play a crucial role in determining the possible signatures of these fermions at colliders.

Fermions get their masses via their interactions with Higgs fields. The relevant Yukawa Lagrangian is noted below:

$$\begin{aligned} \mathcal{L}_{\text{Yukawa}} =\ & y_{qij}\bar{Q}_{iL}\Phi_B Q_{jR} + \tilde{y}_{qij}\bar{Q}_{iR}\tilde{\Phi}_B Q_{jL} + y_{lij}\bar{L}_{iL}\Phi_B L_{jR} \\ & + \tilde{y}_{lij}\bar{L}_{iR}\tilde{\Phi}_B L_{jL} + y_{sij}\bar{Q}_{iLS}\Phi_S Q_{jRS} \\ & + y_{LBij}\text{Tr}[\bar{L}_{iB}\tilde{L}_{jB}]\Phi_S^c + \frac{y_{LSij}}{\Lambda}\bar{L}_{iS}L_{jS}^c\Phi_S\Phi_S \\ & + y_{BBij}\text{Tr}[\bar{L}_{iB}\tilde{\Phi}_B]Ł_{jS}^c + \text{H.c.}, \end{aligned} \tag{33}$$

where i, $j = 1$, 2, 3 are generation numbers and $y(s)$ are Yukawa coupling constants. Φ_S^c is a complex conjugate of Φ_S and $\tilde{L}_B = \sigma_2 L_B^* \sigma_2$.

In general the Yukawa coupling matrices, y_q, y_l, y_{LB}, y_s are nondiagonal.[6] The diagonalization of the Yukawa matrices in the first line of Eq. (33) will give rise to the SM-fermion masses and mixing in the form of V_{CKM} and V_{PMNS}. There are no term present in the Yukawa Lagrangian leading to exotic fermion SM-fermion mixing. Thus while considering the phenomenology of the some of the exotic fermions, we have used their physical masses as the free parameters of the analysis and derive possible bounds on them from LHC itself. The last term in Eq. (33) introduces a mixing between the singlet lepton and the neutral lepton from the bidoublet. In this work, we shall not be investigating the phenomenological implications of this term.

It is important to note a dimension-four mass term for the singlet lepton L_S (a Weyl spinor) cannot be written as it transform nontrivially under $U(1)_{L,R}$. Using the singlet

---

[5]We have only noted a possible Dirac mass term for the neutrinos in Eq. (33).

[6]In general, in an unifying model like E_6, all the Yukawa couplings at the low energy will be generated from a single (and possibly a nondiagonal) Yukawa texture at the GUT scale [24].
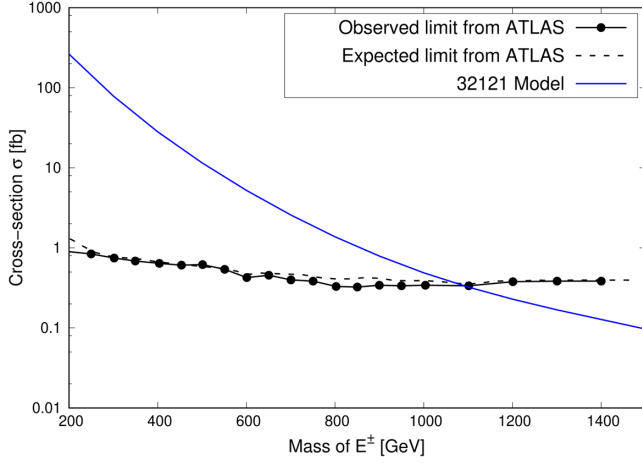
FIG. 6. Observed (line with dots) and expected (dashed) 95% CL experimental upper limit on the cross section (σ) of heavy charged lepton pair production at the 13 TeV run of the LHC. Also shown in the plot the theoretical prediction from the 32121 model (blue line).

Higgs field Φ_S, we are able write a dimension-five operator, which in turn generates mass for L_S. It is well known that any one of the Higgs bosons from **27**-plet of E_6 cannot give mass to L_S. To generate a mass using Higgs mechanism, one must employ a Higgs from a multiplet of E_6 other than **27** [25]. So Λ may be identified with the VEV of such a Higgs boson. Or we can simply assume that L_S has acquired mass from a Higgs belonging to other rep. of E_6, and we treat its mass as a free parameter in our analysis.

One can constrain the masses/Yukawa couplings of exotic quarks and leptons from the direct search limits on their masses at the LHC [26,27]. As for example, the ATLAS collaboration has searched for s long-lived heavy charged lepton at the 13 TeV run with a collected luminosity of 36.1 fb^{-1}. We have estimated the pair-production cross section of E^+E^- at the 13 TeV and compared it with the experimental 95% CL upper limit on the same cross section obtained by the ATLAS collaboration. The plots have been presented in Fig. 6. One can see that the E mass in the 32121 model cannot be less than 1.091 TeV at 95% CL

III. PHENOMENOLOGY OF NEW HIGGS BOSONS OF 32121 MODEL AT THE LHC

Apart from the SM-like Higgs boson, the 32121 model contains a number of neutral and charged scalar states. We will now discuss the possible interactions and signatures of such states at the LHC in this section.

A. Phenomenology of the scalars arising from the bidoublet in the 32121 model

h_2^0 (ξ_2^0) is the neutral CP-even (odd) scalar originating from the Higgs bidoublet, Φ_B. From Eqs. (19) and (20), we
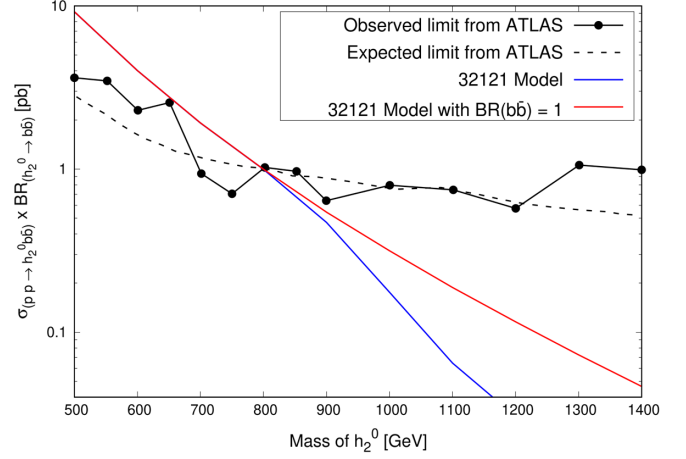

FIG. 7. The black solid (dashed) line represents the observed (expected) 95% CL upper limit on the production cross section (σ) times branching ratio to $b\bar{b}$, of heavy neutral Higgs boson in association with b quarks as a function of Higgs boson mass at $\sqrt{s} = 13$ TeV with 27.8 fb^{-1} integrated luminosity. The blue line corresponds to $\sigma(pp \to h_2^0 b\bar{b}) \times \mathrm{BR}(h_2^0 \to b\bar{b})$ whereas the red line represents the same but considering $m_{H_1^\pm} > mh_2^0$.

can easily see their masses are equal. They do not decay to a pair of gauge bosons as the VEV k_2 has been set to zero. For the very same reason, h_2^0 or ξ_2^0 does not couple to a pair of any other scalars.

h_2^0 (ξ_2^0) couples to a pair SM fermions via Yukawa coupling [see Eq. (33)]. It is interesting to note that the coupling of h_2^0 (ξ_2^0) to a pair of top quarks is proportional to bottom-Yukawa coupling and vice versa. ATLAS and CMS have searched for a heavy neutral Higgs boson produced in association with b quarks followed by its decay to a pair of b quarks at $\sqrt{s} = 13$ TeV [28,29]. We consider the production of an h_2^0 in association with a pair of b quarks and its decay to a pair of b quarks. The resulting rate of events can be compared with the measured rate by the ATLAS collaboration to set a lower limit on the mass of $h_2^0(\xi_2^0)$. The calculated (in 32121 model) and (95% CL upper limit on the) measured cross sections are presented in the Fig. 7. The 95% CL lower limit on $m_{h_2^0/\xi_2^0}$ comes out to be greater than 800 GeV. While estimating the h_2^0 (ξ_2^0) production cross section in association with a pair of b quarks, we have incorporated the QCD K factor (~ 1.1) following the Refs. [30,31]. However, the lower limit derived in the above depends on the charged Higgs boson ($H_1^\pm$) mass in the following way. A careful look into the branching ratios of h_2^0 reveals that it dominantly decays to a pair of b quarks, unless a decay to $H_1^\pm W^\pm$ is kinematically allowed. Consequently, the mass of $H_1^\pm$ plays a crucial role in determining the rate of $4b$ final state from considered above. A heavier charged Higgs (when $h_2^0 \to H_1^\pm W^\mp$ is disallowed) will push the lower limit on the h_2^0 mass in the upward direction and vice versa.

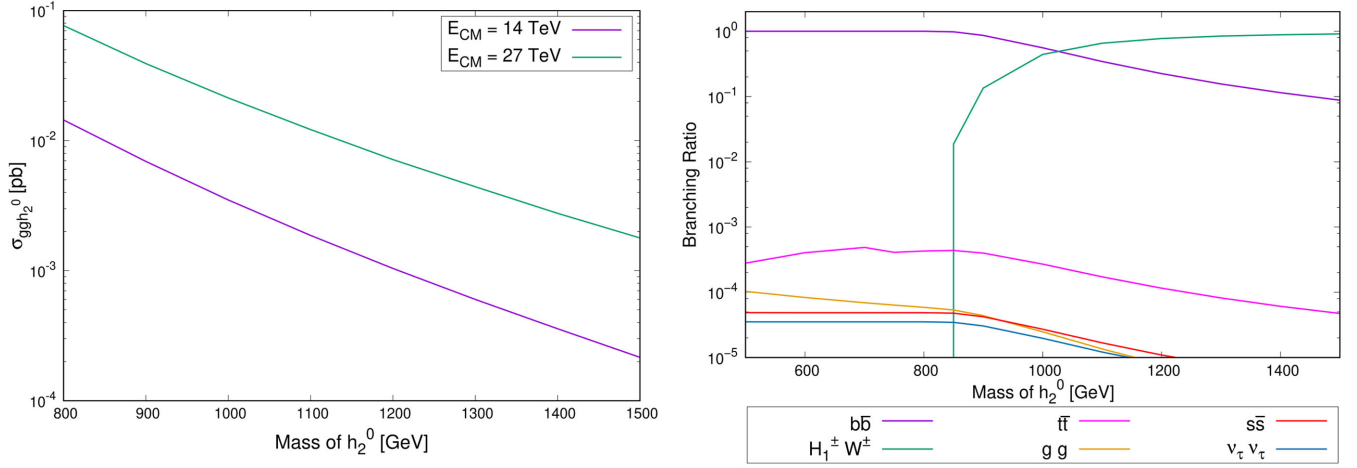FIG. 8.　h_2^0 production cross section (σ) via gluon fusion at LHC (left panel) for the 14 and 27 TeV proton proton center-of-mass energy. The right panel shows the branching ratios of h_2^0 to different final states. h_2^0 and ξ_2^0 have the same masses and coupling strengths.

In Fig. 7, we have presented the $\sigma(pp \to b\bar{b}h_2^0) \to$ $b\bar{b}(b\bar{b})$ in two cases. The red line represents the rate when $m_{H_1^\pm} > m_{h_2^0}$ and the later decays to a pair of $b\bar{b}$ with 100% BR. While the blue curve represents the case when h_2^0 can also decay to $H_1^\pm$, thus having a reduced decay rate to $b\bar{b}$. A charged Higgs mass of 750 GeV has been assumed while making this plot. The sudden change in the slope of the blue curve due to onset of $h_2^0 \to H_1^\pm W^\mp$ decay mode around $m_{h_2^0} \simeq 850$ GeV (see Fig. 8) is evident.

A dominant production mechanism for such a Higgs boson at the LHC will be via gluon gluon fusion (Fig. 9). Unlike the SM Higgs boson, in this case, the gluon gluon fusion cross section is dominated by the bottom quark loop. We present the production cross section [considering next-to-leading order (NLO) QCD correction for this production process, see Ref. [32]] and decay branching ratios of h_2^0 in Fig. 8.

At the 14 TeV run of the LHC, the h_2^0 production cross section varies from 14 fb for $m_{h_2^0} = 800$ GeV to 0.2 fb for 1.5 TeV mass of this scalar. Production cross section at 27 TeV is even higher and it varies from 77 fb at $m_{h_2^0} = 800$ GeV to 1.5 fb for $m_{h_2^0} = 1500$ GeV. Once produced, h_2^0 dominantly decays to a pair of b quarks, unless it decays
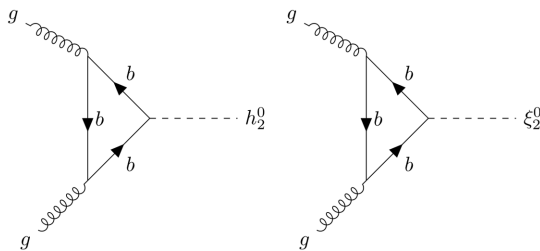
to $H_1^\pm W^\mp$. The later decay mode will only be allowed when $m_{h_2^0}$ is sufficiently higher than $m_{H_1^\pm} + m_W$. This choice of mass ordering depends on the choice of parameters namely λ_3 and $c_4 - c_3$. In the plot presented in Fig. 8, a certain choice of these parameters has been assumed, so $h_2^0 \to H_1^\pm W^\mp$ has been kinematically allowed, with an additional assumption about the mass of $H_1^\pm$ (750 GeV).

In the pseudoscalar sector, ξ_2^0 arises from the Higgs bidoublet and has a mass equal to the mass of h_2^0. It has exactly the similar coupling strengths to the SM fermions as the h_2^0. The choice of vanishing k_2 forbids its coupling to a pair of gauge bosons or the scalars. Consequently the production and decay mechanism and their rate of ξ_2^0 is exactly the same as h_2^0. We will not present these numbers separately.

With charged Higgs boson, $H_1^\pm$ arises from the Higgs bidoublet, Φ_B. From the expression (21), one can see $m_{H_1^\pm}^2 = \frac{1}{2}(c_4 - c_3)(k_1^2 + v_R^2)$. This massive charged Higgs couples to SM fermions and decays to a top and a bottom quark with a nearly 100% branching ratio. It also couples to the heavy gauge bosons of the 32121 model, but the coupling of $H_1^\pm$ to the SM gauge bosons ($W^\pm, Z$) is proportional to k_2, hence it identically vanishes. It can be singly produced at LHC with a top and bottom quark or pair-produced via Drell-Yan process or via vector boson fusion process.

In Fig. 10, we have presented the cross section of associated production of $H_1^\pm$ with a top and a bottom at the LHC and branching ratio of $H_1^\pm$. In the case of $H_1^\pm$ production, the main contribution will be from $gg \to \bar{t}bH_1^\pm$. The ATLAS and CMS collaborations have searched for a heavy charged Higgs boson decaying to a top and bottom at 13 TeV run [33–35]. Using the most recent upper limit on the $\sigma \times BR$ provided by ATLAS, we put a lower limit on the mass of the charged Higgs $m_{H_1^\pm} > 720$ GeV
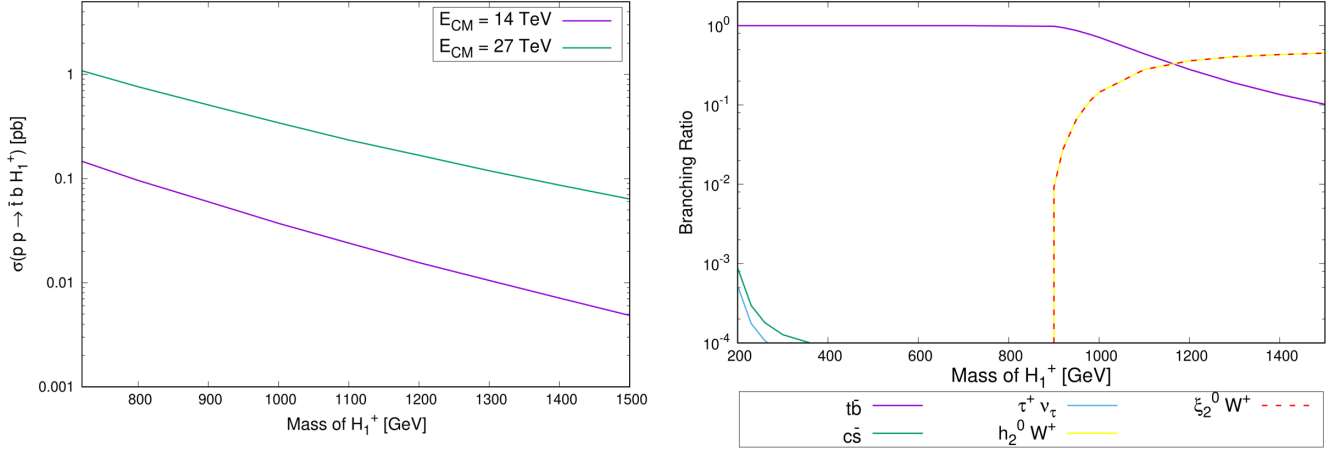

FIG. 9.　Feynman diagrams for h_2^0 and ξ_2^0 production via gluon gluon fusion through a b quark loop.

FIG. 10. $H_1^\pm$ production cross section (σ) via the $pp \to \bar{t}bH_1^+$ process at the LHC (left panel) for the 14 and 27 TeV proton proton center-of-mass energy. The right panel shows the branching ratios of $H_1^\pm$ to different final states setting the mass of $h_2^0(\xi_2^0)$ at its lowest limit (800 GeV).

(see Fig. 11). The sudden change in the slope of the blue curve representing $\sigma(pp \to \bar{t}bH_1^+) \times \mathrm{BR}(H_1^+ \to t\bar{b})$ is due to the sudden decrease of $\mathrm{BR}(H_1^+ \to t\bar{b})$ around $m_{H_1^\pm} = 900$ GeV (see Fig. 10). We have set the mass of $h_2^0(\xi_2^0)$ at its lower limit of 800 GeV following the Fig. 8 corresponding to the scenario when $m_{H_1^\pm} > m_{h_2^0}$ (the red line).

We have presented the cross section for $H^\pm tb$ production (in this process NLO QCD correction and running mass for the b quark can be important, see Refs. [31,36]) at the center-of-mass energies of 14 and 27 TeV. In Fig. 10, the right panel shows the branching ratios of $H_1^\pm$ to different final states. Until kinematically allowed for the decay to

$h_2^0 W^+$ and $\xi_2^0 W^+$, H_1^+ dominantly decays to $t\bar{b}$ ($\mathrm{BR}(H_1^+ \to t\bar{b}) \sim 0.999$). For large $m_{H_1^\pm}$ the branching ratios to $h_2^0(\xi_2^0)W^+$ channel become more dominant.

The cross section for $H^\pm tb$ production at center-of-mass energy approximately 14 (27) TeV varies from 0.15 (1) pb for $m_{H_1^\pm} = 720$ GeV to 0.005 (0.06) pb for $m_{H_1^\pm} = 1500$ GeV. After being produced, $H_1^\pm$ will decay further, and considering respective decay channels [e.g., tb or $h_2^0(\xi_2^0)W^\pm$] one can expect a good amount of events at the HL-LHC. However, one needs to consider further decays of top or $h_2^0(\xi_2^0)$.

B. Phenomenology of the scalars arising from a left-handed Higgs doublet

In this section, our primary concern will be the neutral and charged states originating from the left-handed doublet scalar. Among the neutral CP-even scalar h_L^0, neutral CP-odd scalar ξ_L^0, and charged scalars $H_L^\pm$, The first two have equal masses [see Eqs. (19)–(21)] and do not mix with other neutral states. These three states can be pair produced at the LHC via quark antiquark fusion mediated by one of the electroweak gauge bosons. However as we set v_L to be zero, neither of these states decays to a pair of SM particles.

As already pointed out, we will not vary all the parameters of the mass matrix independently to study the masses of the scalars. We will treat the physical masses as free parameters of our analysis. However some caveats are to be imposed on some combinations of parameters of the mass matrices. As for example, $\rho_3 - 2\rho_1$ will always assumed to be a positive quantity that is ascertained from the positivity of charged Higgs boson ($H_L^\pm$) mass (squared). Now the other charged Higgs boson ($H_1^\pm$) mass squared is proportional to $c_4 - c_3$. This in turn forces us to take this combination also to be positive. As a consequence, masses of h_L^0 and ξ_L^0 are always greater than mass of H_L^+. However
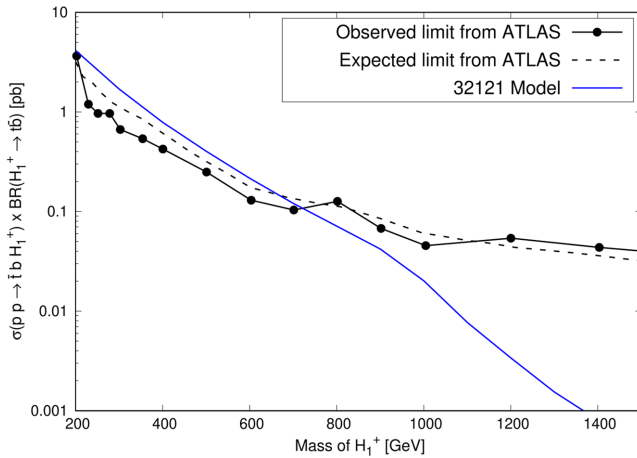

FIG. 11. The black solid and dashed line represent observed and expected 95% CL experimental upper limit on the cross section (σ) times BR of heavy charged scalar production via $pp \to \bar{t}bH_1^+ \times \mathrm{BR}(H_1^+ \to t\bar{b})$ at the 13 TeV run of the LHC with 139 fb^{-1} integrated luminosity [33]. Also shown in the plot the theoretical prediction of $\sigma \times BR$ for H_1^+ production in the 32121 model (blue line).
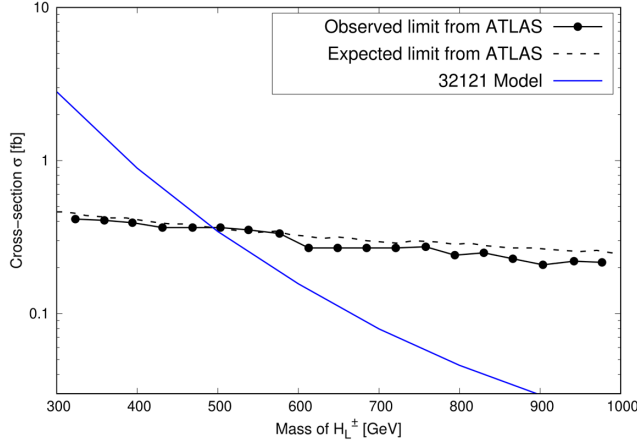
FIG. 12. Observed (line with dots) and expected (dashed) 95% CL experimental upper limit on the cross section (σ) of heavy stable charged scalar pair production at the 13 TeV run of the LHC. Also shown in the plot is the theoretical prediction for the $H_L^+ H_L^-$ pair-production cross section in the 32121 model (blue line).

$(m_{h_L^0} - m_{H_L^+})$ can be controlled by choosing a proper magnitude of the combination $(c_4 - c_3)\frac{k_1^2}{2}$. From the expressions (19) and (21), $m_{h_L^0}^2 = (c_4 - c_3)\frac{k_1^2}{2} + m_{H_L^\pm}^2$. We will see in the following that h_L^0 will decay to $H_L^+ W^-$ if kinematically allowed. So in order to make h_L^0 stable, one needs to set $(c_4 - c_3)\frac{k_1^2}{2} < m_W^2 + 2 m_W m_{H_L^\pm}$. However, an unstable h_L^0 implies that the mass of $H_1^\pm$ becomes too heavy in the ballpark of 17 TeV.

In the following analysis, h_L^0 and ξ_L^0 are assumed to be stable. Thus they could be potential candidates for DM. $H_L^\pm$ also does not have any decay mode. Once produced at colliders, it passes through the detector without

decaying. However being a charged particle, it leaves its signature in the tracker and electromagnetic (e.m.) calorimeter before leaving the detector. The ATLAS collaboration has searched for long-lived stau ($\tilde{\tau}$, the super-symmetric partner of the τ lepton), which are very similar to the $H_L^\pm$ [27]. So the upper limit of the cross section of pair production of such long-lived $\tilde{\tau}$ s at the LHC center-of-mass energy of 13 TeV, as quoted by the ATLAS collaboration, can be used in our case to constrain the $m_{H_L^\pm}$, which is the only free parameter that controls the $H_L^\pm$ pair production. In Fig. 12, we present the variation of $H_L^\pm$ pair-production cross section (blue solid line) as a function of its mass. Overlaid are the observed and expected upper limits on the pair production of long-lived stau (black solid and dashed lines). The intersection of these two curves gives us a 95% CL lower limit of 494 GeV, on the left-handed charged Higgs boson ($H_L^\pm$) mass.

Let us now concentrate on the possible production and decay signatures of charged and neutral Higgs bosons arising from the left-handed doublet. As mentioned above, these can be pair-produced at the LHC via a mechanism similar to the Drell-Yan one. In Fig. 13, the pair-production cross sections have been presented with Higgs masses at the 14 (27) TeV run of LHC. One can see from Fig. 13, production cross section for $H_L^\pm$ varies from 0.4 (1.8) fb at 500 GeV to 0.005 (0.06) fb at 1.5 TeV at the center-of-mass energy 14 (27) TeV. $H_L^\pm$ being stable does not decay any further and we are left with two ionizing tracks of heavy particles in the detector [27,37]. At HL-LHC, such a cross section results into 15 background free events even for a $H_L^\pm$ mass of 1.5 TeV. This particular signature is unique and cannot arise from the SM. Thus we hope to explore stable charged Higgs masses up to 1.5 TeV at the 14 TeV HL run of LHC.
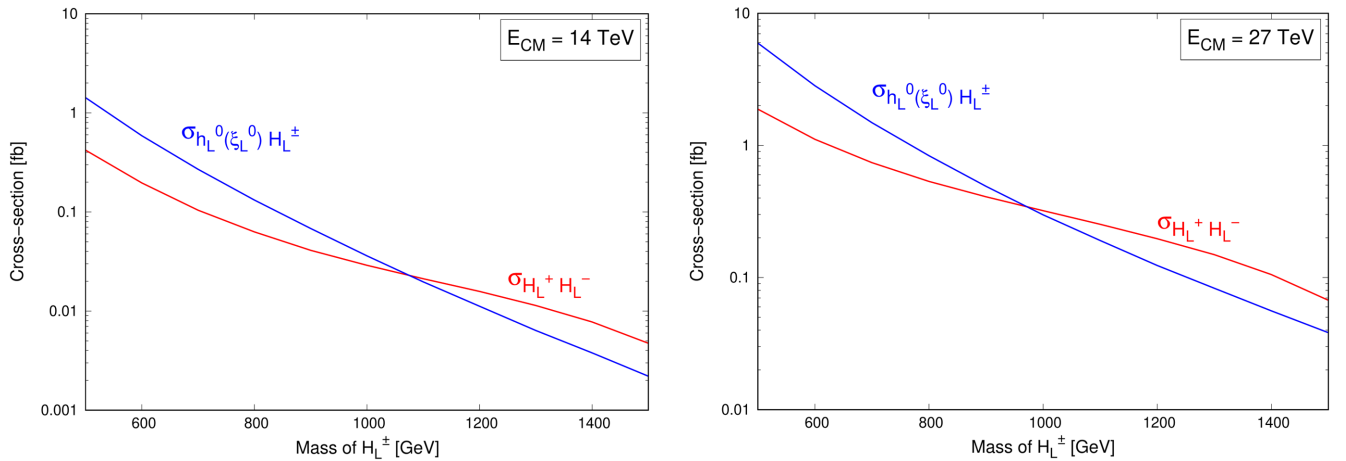

FIG. 13. The red solid line corresponds to the $H_L^\pm$ pair-production cross section (σ) at LHC at $\sqrt{s} = 14$ TeV (left panel) and at $\sqrt{s} = 27$ TeV (right panel), whereas the blue solid line represents the combined production cross section of one charged ($H_L^\pm$) and one neutral (*CP*-even or *CP*-odd) scalar at LHC at $\sqrt{s} = 14$ TeV (left panel) and at $\sqrt{s} = 27$ TeV (right panel).
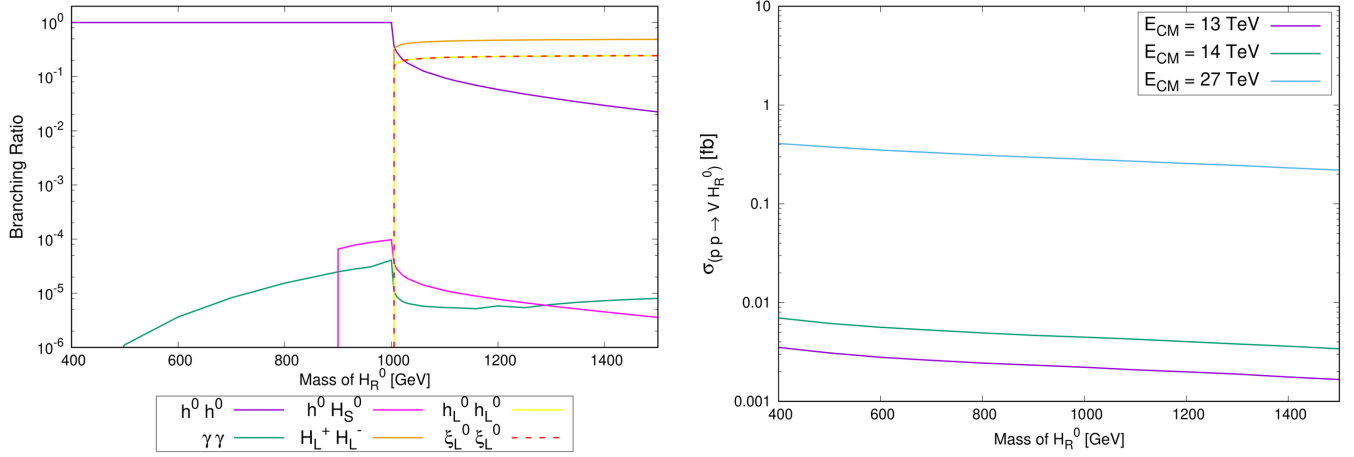
FIG. 14. Associated production cross section (σ) of H_R^0 along with a vector boson at LHC (left panel) for 13, 14, and 27 TeV proton proton center-of-mass energy. The right panel shows the branching ratios of H_R^0 to different final states with an assumption of $m_{h_L^0} = m_{\xi_L^0} = 500$ GeV and $m_{H_S^0} = 700$ GeV.

We now turn to the production of a $H_L^\pm$ in association with either a h_L^0 or ξ_L^0. The production mechanism at the LHC is same as above but with a small difference. The scalar current in the later case is connected to initial state left-handed quark current by a $W^\pm$ propagator. Consequently the cross section for $h_L^0 H_L^\pm$ is lower than the $H_L^\pm$ pair production. However, when we combine the $\xi_L^0 H_L^\pm$ with it, the total cross section of associated production becomes comparable with the pair-production rate of charged Higgs bosons. In Fig. 13, the associated production cross section has been presented. One can see that at the 14 (27) TeV run of LHC, the cross section varies from 1.4 (5.9) fb to 0.002 (0.038) fb when the charged Higgs mass varies from 0.5 to 1.5 TeV.

While discussing the possible signatures of the associated production, we have to be careful about the mass ordering between H_L^+ and $h_L^0(\xi_L^0)$. When kinematically allowed, h_L^0 will decay (with 100% branching ratio) to $W^- H_L^+$. Depending the further decay of the W boson, associated production will result into two charged tracks +2 jets or two charged tracks with a lepton and $\not{E}_T$. On the other hand when h_L^0 is stable, the associated production would result into a signal, comprising of a single charged track (from $H_L^\pm$) in association with $\not{E}_T$ (arising from h_L^0 and ξ_L^0).

C. Phenomenology of the scalar arising from right-handed Higgs doublet

Next, in our agenda is the heavy neutral Higgs boson, H_R^0. Due to nonzero v_R, it couples to a pair of neutral heavy gauge bosons. But it cannot have any coupling to SM fermions.[7] The plot (Fig. 14) showing the branching ratios of H_R^0 reveals that it dominantly decays to a pair of SM

Higgs bosons or to a pair of $H_L^\pm$ or $h_L^0(\xi_L^0)$ once these decays are kinematically allowed. Decay to a pair of heavy neutral gauge bosons are kinematically disallowed. Furthermore, the coupling of H_R^0 to a pair of Z bosons conspires to be small hence its decay rate to a pair Z bosons is negligible. H_R^0 can have an effective coupling at one loop ($H_L^\pm$, $W_R^\pm$, and $H_1^\pm$ running in the triangle loop) to a pair of photons. The decay branching ratio can be as high as 10^{-5} over a wide mass range of H_R^0 and is thus not phenomenologically very interesting.

The main production mechanism for H_R^0 is in association with a gauge boson (Z, Z', A', and W_R) via the annihilation of a quark antiquark pair. It can also be produced in vector boson fusion mechanism. In this article, we will only consider the production of H_R^0 in association with a vector boson (Fig. 15).

In Fig. 14 (right panel) we have presented the combined cross section of production of a H_R^0 in association with Z', A', and W_R, with the heavy gauge boson masses set at their experimental lower limits. Among these three production channels, contribution of $\sigma(H_R^0 A')$ is nearly 70% of combined cross section presented in Fig. 14. The combined
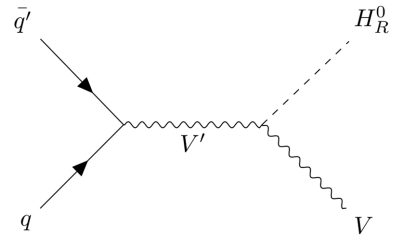

FIG. 15. Feynman diagram for H_R^0 production in association with a vector boson where V, V' represent any vector boson of 32121 model (Z, Z', A', and W_R).

---

[7]It may couple to the SM fermions if we allow a possible mixing between H_R^0 with SM Higgs boson.

cross section of H_R^0 associated production at the LHC varies from 0.4 to 0.22 fb for a range of m_{H_R} : 400 to 1500 GeV at a center-of-mass energy of 27 TeV. At the 14 TeV run of the LHC, the cross section is quite small. It is in the ballpark of 0.005 fb (Fig. 14) for a H_R^0 of 1 TeV mass. The kinematic suppression due to the presence of a heavy gauge boson in the final state can be one of the reasons behind the smallness of the total cross section.

Before we close this subsection, let us make some brief comments about the possible signature of H_R^0 at the LHC. The most promising signature in our opinion will arise when H_R^0 can decay to a pair of $H_L^\pm$s. As mentioned before, it will produce two charged tracks in the detector with their invariant mass peaking at the mass of H_R^0. Along with a pair of charged tracks heavy gauge boson decay will probably give rise to a pair of high mass jets or leptons. As for example, at the 27 TeV run of the HL-LHC, one expects around 30 two charged tracks two lepton events for a $m_{H_R^0} = 1$ TeV.[8] While at the 14 TeV run with the high luminosity option, detection of such events seems to be very challenging even for a 500 GeV H_R^0.

D. Phenomenology of the $SU(2)_L \otimes SU(2)_R$ singlet scalar in the 32121 model

Next, in our agenda, is the scalar arising from the $SU(2)_L \times SU(2)_R$ singlet Φ_S. β_1 being small in order to satisfy the SM Higgs bosons signal strength (see Fig. 1), it does not have any significant role in the phenomenology of the singlet scalar and we can treat the mass of the singlet scalar itself as the free parameter of our analysis. In the following we intend to study the decays and dominant production channel of the singlet scalar boson.

In Fig. 16, we present branching ratios of H_S^0 to its available decay channels. As a reminder, WW, ZZ, $t\bar{t}$, $b\bar{b}$ decays of H_S^0 take place via the mixing with the SM Higgs boson. While rest of the decays are driven via the direct couplings of H_S^0 to the decaying particles.

The dominant contribution to the $H_S^0 \to gg, \gamma\gamma$ decay arises from triangle loops of heavy exotic quarks and leptons. Charged Higgs states arising from Φ_B, Φ_L also contribute to singlet Higgs decay to $\gamma\gamma$. $H_S^0 \to gg$ is important as a production cross section of H_S^0 via gluon
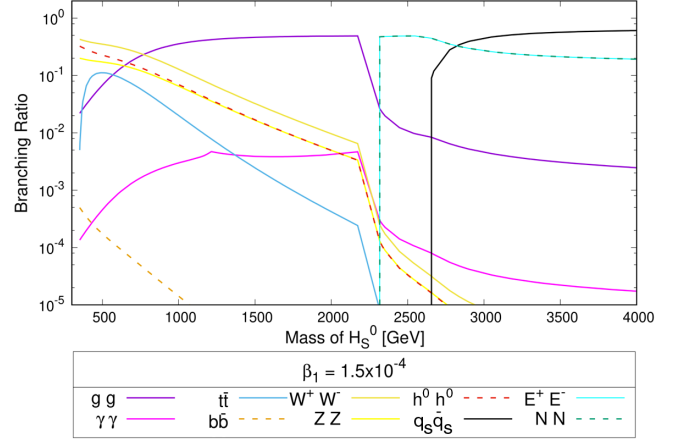

FIG. 16. Branching ratio of H_S^0 to different channels including exotic quarks and exotic leptons for $\beta_1 = 1.5 \times 10^{-4}$ and $v_S = 13$ TeV and exotic quark mass 1.3 TeV.

fusion is directly proportional to this decay width. However, v_S being large, singlet Higgs Yukawa to exotic leptons/quarks are tiny [see Eq. (33) in Sec. II C]. Consequently, decay width to gg is small. Similar arguments can be given to understand the smallness of $H_S^0 \to \gamma\gamma$ decay rate.

The branching ratios to several decay channels are moderately sensitive to β_1. With a higher value of $\beta_1(\sim 10^{-3})$ one can satisfy all the constraints from the SM Higgs boson signal strengths. However, $\beta_1 > 10^{-39}$ will lead to a singlet Higgs boson mass of 700 GeV and above. Furthermore, a higher value of β_1 leads to a larger mixing between the singlet and the SM-like Higgs boson. Thus the singlet Higgs boson decay rates to tt, bb, WW, and ZZ channels will increase slightly. The variation of branching ratios over a wide mass range of H_S^0 for a fixed β_1 have been shown in the Fig. 16.

In this section we present singlet Higgs production cross section via gluon gluon fusion over a range of singlet Higgs mass. The production mechanism is the same as the SM Higgs production via gluon fusion. However, the triangle loop (see Fig. 17) is driven by exotic quarks, which are heavy in mass. There will be a very tiny contribution from the Standard Model top quark through the mixing of singlet Higgs with the SM Higgs boson. While estimating this cross section we have incorporated a K factor following Ref. [32], assuming a higher order QCD correction to the production of a singlet Higgs boson will be of similar order

---

[8]The branching ratio for dilepton decay (e, μ, τ) of A' is ~10% and the branching ratio of $H_R^0 \to H_L^+ H_L^-$ is around 50%. So considering an almost 70% contribution of $\sigma(H_R^0 A')$, at the 27 TeV run with 3000 fb^{-1} integrated luminosity, for the process $\sigma(pp \to H_R^0 A') \times \text{BR}(A' \to ll) \times \text{BR}(H_R^0 \to H_L^+ H_L^-)$ one can expect around 30 events for 1 TeV H_R^0 mass.

[9]$\beta_1 > 0.01$ is excluded as the singlet component in SM-like Higgs will be too high to satisfy the experimentally measured signal strengths.
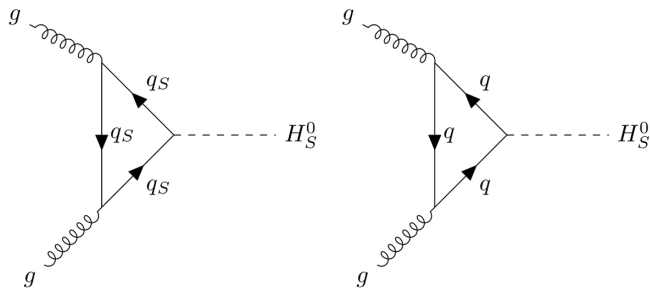
FIG. 17.   Feynman diagram for H_S^0 production via gluon gluon fusion quark loops, q_S is the exotic singlet quark and q represents any SM quark.

to that of a SM Higgs boson production via gluon fusion. For our illustration we have assumed β_1 (mixing parameter) to be equal to 1.5×10^{-4}. This value of β_1 is consistent with the measured values of SM Higgs boson signal strengths to different channels.

In Fig. 18, we have presented the singlet Higgs boson production cross section at the proton proton center-of-mass energies 13, 14, and 27 TeV, respectively. At the 14 (27) TeV run of LHC, production cross section varies from 15.9 (57.6) fb to 10^{-3} (0.056) fb when H_S^0 mass changes from 0.3 to 4 TeV. Although the production mechanism is similar to the SM Higgs boson production via gluon fusion, the cross section for H_S^0 production is order of magnitude smaller than a SM-like Higgs boson of same mass, even after considering the contribution from three species of $SU(2)$ singlet exotic quarks. This can be explained by the small Yukawa coupling of these
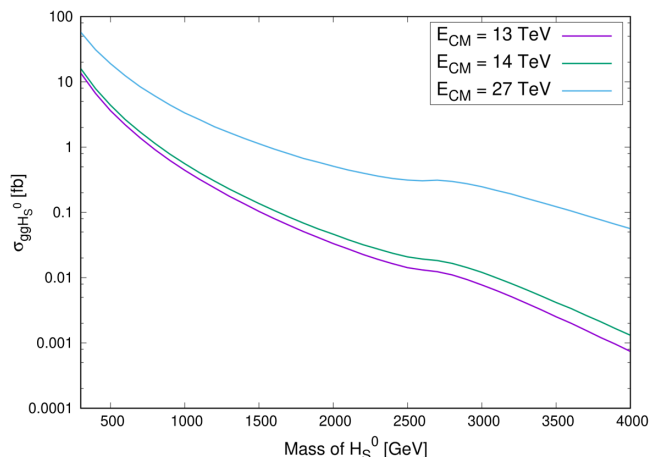

FIG. 18. H_S^0 production cross section (σ) via gluon fusion for $\beta_1 = 1.5 \times 10^{-4}$ and $v_S = 13$ TeV and exotic quark mass 1.3 TeV.

exotic quarks to the singlet Higgs boson [see Eq. (33)]. We have assumed the exotic quark mass to be equal to 1.3 TeV [26].[10] Before we conclude, let us make some qualitative comments about the possible signatures of H_S^0 at the LHC. For a low mass (<700 GeV), the WW decay mode can be exploited to look for possible signatures of this Higgs boson. However, once $m_{H_S^0}$ becomes greater than a TeV, the gluon gluon decay of H_S^0 becomes dominant and detection of such a scalar will be difficult due to a possible large QCD background. However, for higher singlet Higgs masses (>2.2 TeV), it can decay to a pair of exotic leptons, thus it will produce a unique signature of two charged tracks with their invariant mass peaking at the singlet Higgs mass. This signal will be background free and probably the best bet for detection of such a scalar boson. As, for example, at the 14 TeV LHC, decay of a 2.2 TeV H_S^0 will approximately produce 48 events with a pair of charged tracks with 3 ab^{-1} integrated luminosity. While we expect to have 15 such events for a 3 TeV H_S^0 at the 14 TeV run with the same luminosity. At the 27 TeV run, the situation will improve drastically, and we can expect to see 80 such events even for a 4 TeV singlet Higgs boson.

Finally we would like to make a brief comment about the situation when $c_1 + c_3 \neq 0$ and $\gamma_1 \neq 0$. Making $c_1 + c_3$ nonzero would introduce mixing between right-handed neutral scalar with SM-like Higgs boson. However, we have to satisfy the experimentally observed signal strengths of h^0. This in turn limits the above mixing and the H_R^0 would possibly have small decay channels to the SM fermions and SM gauge bosons. On the other hand a nonzero γ_1 would have a more prominent effect on $H_R^0 - H_S^0$ phenomenology. A γ_1 induced mixing between H_R^0 and H_S^0 would lead to H_R^0 decays to SM fermions along with exotic fermions when kinematically allowed. At the same time, both these states could be produced via gluon fusion.

The production of the BSM scalars in 32121 model and the possible backgrounds are discussed in Table III very briefly.

---

[10]The lower limit on the mass of a heavy stable quark following the Ref. [26] is 200 GeV, obtained from the 8 TeV run of the LHC. Due to the nonavailability of any further updated analysis at 13 TeV, we have assumed that mass limit, on such an object, is in the ballpark of a TeV. The mass limit on heavy stable lepton [27] is 1.09 TeV. Assuming that the quarks will have a higher production cross section at the LHC, we have assumed they must be heavier than the exotic leptons.

TABLE III.   Significant production processes of BSM scalars of 32121 at the LHC and their possible backgrounds.

Scalars	Production at LHC	Possible final state	Possible backgrounds
$h_2^0(\xi_2^0)$	$h_2^0(\xi_2^0)b\bar{b}$	$b\bar{b}b\bar{b}l^+l^-\nu_l\bar{\nu}_l$	$t\bar{t}b\bar{b}, t\bar{t}h$, DY + jets
$H_1^\pm$	$H_1^+\bar{t}b$	$b\bar{b}b\bar{b}l^+l^-\nu_l\bar{\nu}_l$	$t\bar{t}b\bar{b}, t\bar{t}h$, DY + jets
$H_L^\pm$	$H_L^+H_L^-$ pair production	$H_L^+H_L^-$	Stable heavy charged particle creating two charged tracks and possibly background free
	$H_L^+h_L^0(\xi_L^0)$	$H_L^+h_L^0(\xi_L^0)$	Being stable and neutral $h_L^0(\xi_L^0)$ will remain undetected and H_L^+ will create one charged track and possibly background free
H_R^0	H_R^0A'	$H_L^+H_L^-l^+l^-$	Two oppositely charged tracks of heavy stable particles, invariant mass distribution of $H_L^+H_L^-$ should peak at $M_{H_R^0}$, background free
H_S^0	H_S^0 via gluon fusion	E^+E^-	Stable heavy charged particle creating two charged tracks and possibly background free
		$q_S\bar{q}_S$	Stable heavy charged colored particles will hadronize

IV. CONCLUSIONS

To summarize, we have investigated phenomenological implications of a LR symmetric model based on a E_6 inspired gauge group $SU(3)_C \otimes SU(2)_L \otimes U(1)_L \otimes SU(2)_R \otimes U(1)_R$. The later symmetry group can be a result of two step breaking of E_6. We have studied the phenomenology of the Higgs bosons, responsible for the symmetry breaking of 32121 gauge group down to the SM gauge group. The model is hallmarked by the presence of a complete family of **27**-plet of fermions belonged to the fundamental representation of E_6. Apart from these TeV scale fermions, a weak bidoublet [under $SU(2)_L \times SU(2)_R$], a right-handed Higgs doublet and a singlet is necessary for complete symmetry breaking. The measured value of the W-boson mass fixes one of the bidoublet vacuum expectation values, which we identify with the SM Higgs VEV. The experimental lower limits on the mass of right-handed charged gauge boson W_R in turn constrain the vacuum expectation value, v_R, of the neutral member of the right-handed Higgs doublet. v_R comes out to be greater than 14 TeV. The second bidoublet VEV k_2 is set to zero to avoid a possible admixture of W_R in the SM W boson. Appearance of an additional massive neutral gauge boson is a result of the breaking of an extra $U(1)$ symmetry. The experimental lower limit from the LHC, on the mass of such an extra $U(1)$ gauge boson puts a lower limit of 12.61 TeV on the vacuum expectation value v_S of the singlet scalar boson.

All fermions present in the 27-dimensional fundamental representation of E_6 are considered to be present in our model. We have written down the relevant dimension-four Yukawa interactions of these fermions either with the bidoublet scalar or the singlet scalar field, excepting the singlet lepton field L_S, for which we write a dimension-five Yukawa term involving singlet scalar Φ_S.

Furthermore, using the LHC data on the search of heavy charged long-lived particles, we have put a lower limit of 1.09 TeV on the mass of heavy exotic charged lepton.

After discussing the symmetry breaking pattern in some details, we have mainly devoted ourselves on the phenomenology of the scalars (*CP*-even, *CP*-odd, and charged Higgs) present in this model. We investigated their decay modes, and possible production processes at the LHC. Without going into the details of signal background analysis we have discussed possible signatures of the Higgs bosons arising from this model.

Apart from the SM-like Higgs boson h^0, two more neutral scalars (h_2^0 and ξ_2^0) of same mass and having similar couplings to the SM fermions will originate from the bidoublet after SSB. Lower limit on the masses of these scalars have been obtained from the LHC data and they must be heavier than 800 GeV. Their dominant production mechanism at the LHC will be in association with a pair of b quarks. Once produced they will mainly decay to a pair of b quarks. The production cross section of such scalars via gluon fusion vary from 14(77) fb to 0.2 (1.5) fb for $m_{h_2^0} = 800$ and 1500 GeV, respectively, at 14 (27) TeV run of LHC.

Three more neutral Higgs bosons arise after SSB from the left- and right-handed doublets. Two of them have their origin in the left-handed doublet and one in the right-handed doublet. The neutral Higgses originating from the left-handed doublet are stable and once produced in the collider they can only contribute to the missing energy signature. These scalars can be a good candidate for a relic of the Universe. While the scalar which arise from right-handed doublet can be produced at the LHC in association with any of the neutral gauge boson (Z, Z', or A') or via the vector boson fusion process. The production cross section varies from 0.4 to 0.22 fb for a range of Higgs mass 400 to 1500 GeV.

Two charged Higgs bosons will be the hallmark of the model. One of them, $H_1^\pm$, comes from the bidoublet, and this particular charged state mainly couples to a t and a b quark via Yukawa interactions. A lower limit of 720 GeV has been derived on its mass from the LHC data. The estimated cross section for $H_1^\pm$ production in association with tb varies from 0.15(1) and 0.005(0.06) pb for $m_{H_1^\pm} = 720$ and 1500 GeV, respectively, at the 14 (27) TeV center-of-mass energy at the LHC. The rest of the charged states have an origin in the left-handed doublet. They can be produced at the LHC in a mechanism similar to the Drell-Yan one. Once produced they will not decay. But being charged, they will leave their signature in the detector via an ionizing track. In supersymmetry (SUSY) models, similar signal are produced by stable/long-lived stau. Such a signal has been looked for at the LHC by the ATLAS collaboration. A lower limit on the mass of the charged Higgs $H_L^\pm(>494)$ GeV has been derived using the ATLAS data. We further investigate the pair production of $H_L^\pm$ and associated production of $H_L^\pm H_L^0(\xi_L^0)$ at the LHC.

The last menu in our list is the singlet Higgs. It decays dominantly to a pair gluons and exotic fermions. We consider its production via gluon fusion at the LHC. However, production cross section of a singlet Higgs via gluon fusion is inversely proportional to a singlet VEV, v_S^2. However, v_S being in the ballpark of 13 TeV, singlet Higgs production via gluon fusion fall below the level of a fb for a 1.5 TeV singlet Higgs even at 27 TeV run of the LHC.

Finally we would like to point out that, the Higgs sector of this model promises interesting phenomenology. A detail signal-background analysis has been already in our agenda [38]. Finally, the neutral $SU(2)$ singlet lepton N, Higgs bosons h_L^0 and ξ_L^0 can serve the purpose of relic. It is important to see whether they can satisfactorily fulfil the constraints from the experimental data on relic density and direct detection of dark matter [39].

APPENDIX A: MASSES AND MIXINGS IN THE PARTICLE SECTOR OF THE 32121 MODEL

1. Neutral *CP*-even scalars

$$
\begin{pmatrix} h_1^0 \\ h_2^0 \\ h_L^0 \\ h_R^0 \\ h_S^0 \end{pmatrix} = \begin{pmatrix} \cos\theta & 0 & 0 & 0 & \sin\theta \\ 0 & 1 & 0 & 0 & 0 \\ 0 & 0 & 1 & 0 & 0 \\ 0 & 0 & 0 & 1 & 0 \\ -\sin\theta & 0 & 0 & 0 & \cos\theta \end{pmatrix} \begin{pmatrix} h^0 \\ h_2^0 \\ h_L^0 \\ H_R^0 \\ H_S^0 \end{pmatrix} \tag{A1}
$$

where

$$
\theta = \frac{1}{2}\tan^{-1}\left(\frac{\beta_1 k_1 v_S}{\alpha_1 v_S^2 - \lambda_1 k_1^2}\right).
$$

The basis on the lhs is the gauge eigenstates of the neutral *CP*-even scalars and the basis on the rhs shows the mass eigenstates, where θ is the mixing angle.

2. Charged scalars

$$
\begin{pmatrix} h_1^+ \\ h_2^+ \\ h_L^+ \\ h_R^+ \end{pmatrix} = \begin{pmatrix} c_{11} & 0 & 0 & c_{14} \\ 0 & 1 & 0 & 0 \\ 0 & 0 & 1 & 0 \\ c_{41} & 0 & 0 & c_{44} \end{pmatrix} \begin{pmatrix} H_1^+ \\ H_2^+ \\ H_L^+ \\ H_R^+ \end{pmatrix} \tag{A2}
$$

where

$$
c_{11} = \sqrt{1 - \frac{k_1^2}{v_R^2}} = c_{44}, \qquad c_{14} = \frac{k_1}{v_R} = -c_{41}.
$$

3. Neutral gauge sector

$$
\begin{pmatrix} W_{3L} \\ W_{3R} \\ B_L \\ B_R \end{pmatrix} = \begin{pmatrix} a_{11} & a_{12} & a_{13} & a_{14} \\ a_{21} & a_{22} & a_{23} & a_{24} \\ a_{31} & a_{32} & a_{33} & a_{34} \\ a_{41} & a_{42} & a_{43} & a_{44} \end{pmatrix} \begin{pmatrix} Z \\ Z' \\ A' \\ A \end{pmatrix}, \tag{A3}
$$

where A is the photon and a_{ij} are the elements of the mixing matrix or the rotational matrix that rotates the gauge basis to mass basis:

$$a_{11} = \cos\theta_W, \qquad a_{21} = \frac{-g'\sin\theta_W}{g_{2R}}, \qquad a_{31} = \frac{-g'\sin\theta_W}{g_{1L}}, \qquad a_{41} = \frac{-g'\sin\theta_W}{g_{1R}},$$

$$a_{14} = \sin\theta_W, \qquad a_{24} = \sin\theta_W, \qquad a_{34} = \frac{\sqrt{\cos 2\theta_W}}{\sqrt{2}}, \qquad a_{44} = \frac{\sqrt{\cos 2\theta_W}}{\sqrt{2}},$$

$$a_{12} = -1.643\times10^{-4}, \qquad a_{22} = 0.704, \qquad a_{32} = -0.707, \qquad a_{42} = 5.457\times10^{-2},$$

$$a_{13} = 2.255\times10^{-5}, \qquad a_{23} = -0.450, \qquad a_{33} = -0.386, \qquad a_{43} = 0.804.$$

APPENDIX B: COUPLINGS OF THE BSM SCALARS IN THE 32121 MODEL

1. For h_2^0/ξ_2^0

$M_{h_2^0}$ (GeV)	$\frac{1}{\sqrt{2}}\sqrt{4\lambda_3 k_1^2 + (c_4 - c_3)v_R^2}$	$M_{\xi_2^0}$ (GeV)	$\frac{1}{\sqrt{2}}\sqrt{4\lambda_3 k_1^2 + (c_4 - c_3)v_R^2}$
$h_2^0 b\bar{b}$ Coupling	$\frac{y_t}{\sqrt{2}}$	$\xi_2^0 b\bar{b}$	$\frac{y_t}{\sqrt{2}}\gamma^5$
$h_2^0 H^\pm W^\mp$	$\frac{g_{2L}}{2}\sqrt{1 - \frac{k_1^2}{v_R^2}}$	$\xi_2^0 H^\pm W^\mp$	$\frac{g_{2L}}{2}\sqrt{1 - \frac{k_1^2}{v_R^2}}$
$h_2^0 t\bar{t}$	$\frac{y_b}{\sqrt{2}}$	$\xi_2^0 t\bar{t}$	$\frac{y_b}{\sqrt{2}}\gamma^5$

2. For H_R^0

$M_{H_R^0}$ (GeV)	$\sqrt{2\rho_1 v_R^2}$
$H_R^0 h^0 h^0$	$-(c_1 + c_4)\cos^2\theta v_R - \gamma_1 \sin^2\theta v_R$
$H_R^0 H_L^\pm H_L^\mp$	$-\rho_3 v_R$
$H_R^0 h_L^0 h_L^0 / H_R^0 \xi_L^0 \xi_L^0$	$-\rho_3 v_R$
$H_R^0 h^0 H_S^0$	$(\gamma_1 - c_1 - c_4)\sin\theta\cos\theta v_R$

3. For H_S^0

$M_{H_S^0}$ (GeV)	$\sqrt{2\alpha_1 v_S^2}$
$H_S^0 ZZ$	$\left[\frac{g_{2L}^2\cos^2\theta_W k_1}{2} + g_{2L}g'\sin\theta_W\cos\theta_W k_1 + \frac{g'^2\sin^2\theta_W k_1}{2}\right]\sin\theta$
$H_S^0 h^0 h^0$	$-\beta_1\sin^3\theta k_1 + 2(\beta_1 - 3\lambda_1)\sin\theta\cos^2\theta k_1$
	$+2(\beta_1 - 3\alpha_1)\sin^2\theta\cos\theta v_S - \cos^3\theta\beta_1 v_S$
$H_S^0 W^\pm W^\mp$	$\frac{g_{2L}^2\sin\theta k_1}{2}$
$H_S^0 t\bar{t}$	$\frac{y_t\sin\theta}{\sqrt{2}}$
$H_S^0 E^\pm E^\mp (H_S^0 NN)$	$\sqrt{2}y_{LB}\cos\theta$
$H_S^0 q_S\bar{q}_S$	$\frac{y_s\cos\theta}{\sqrt{2}}$

4. For $H_1^\pm$

$M_{H_1^\pm}$ (GeV)	$\frac{1}{\sqrt{2}}\sqrt{(c_4 - c_3)(k_1^2 + v_R^2)}$
$H_1^+ \bar{t}b$	$-(y_t + y_b)\sqrt{1 - \frac{k_1^2}{v_R^2}}$
$H_1^+ h_2^0 W^- / H_1^+ \xi_2^0 W^-$	$\frac{g_{2L}}{2}\sqrt{1 - \frac{k_1^2}{v_R^2}}$

[1] G. Aad *et al.* (ATLAS Collaboration), Observation of a new particle in the search for the Standard Model Higgs boson with the ATLAS detector at the LHC, Phys. Lett. B **716,** 1 (2012).

[2] S. Chatrchyan *et al.* (CMS Collaboration), Observation of a new boson at a mass of 125 GeV with the CMS experiment at the LHC, Phys. Lett. B **716,** 30 (2012).

[3] M. Mühlleitner, M. O. P. Sampaio, R. Santos, and J. Wittbrodt, Phenomenological comparison of models with extended Higgs sectors, J. High Energy Phys. 08 (2017) 132; J. Steggemann, Extended scalar sectors, Annu. Rev. Nucl. Part. Sci. **70,** 197 (2020) and references therein.

[4] C. E. Yaguna, The singlet scalar as FIMP dark matter, J. High Energy Phys. 08 (2011) 060; R. Campbell, S. Godfrey, H. E. Logan, and A. Poulin, Real singlet scalar dark matter extension of the Georgi-Machacek model, Phys. Rev. D **95,** 016005 (2017); The GAMBIT Collaboration, Status of the scalar singlet dark matter model, Eur. Phys. J. C **77,** 568 (2017); P. Das, M. K. Das, and N. Khan, A new feasible dark matter region in the singlet scalar scotogenic model, Nucl. Phys. **B964,** 115307 (2021).

[5] R. N. Mohapatra and P. B. Pal, Massive neutrinos in physics and astrophysics, World Sci. Lect. Notes Phys. **72,** 1 (2004); N. G. Deshpande, J. F. Gunion, B. Kayser, and F. Olness, Left-right-symmetric electroweak models with triplet Higgs field, Phys. Rev. D **44,** 837 (1991); E. Ma and U. Sarkar, Neutrino Masses and Leptogenesis with Heavy Higgs Triplets, Phys. Rev. Lett. **80,** 5716 (1998).

[6] C. Hati, S. Patra, P. Pritimita, and U. Sarkar, Neutrino masses and leptogenesis in left-right symmetric models: A review from a model building perspective, Front. Phys. **6,** 19 (2018).

[7] A. Vicente, Higgs lepton flavor violating decays in two Higgs doublet models, Front. Phys. **7,** 174 (2019); N. Ghosh and J. Lahiri, Revisiting a generalized two-Higgs-doublet model in light of the muon anomaly and lepton flavor violating decays at the HL-LHC, Phys. Rev. D **103,** 055009 (2021); N. Ghosh and J. Lahiri, Generalized 2HDM with wrong-sign lepton Yukawa coupling, in light of $g_\mu - 2$ and lepton flavor violation at the future LHC, Eur. Phys. J. C **81,** 1074 (2021); D. Das, P. M. Ferreira, A. P. Morais, I. Padilla-Gay, R. Pasechnik, and J. P. Rodrigues, A three Higgs doublet model with symmetry-suppressed flavour changing neutral currents, J. High Energy Phys. 11 (2021) 079; S. Iguro, Y. Muramatsu, Y. Omura, and Y. Shigekami, Flavor physics in the multi-Higgs doublet models induced by the left-right symmetry, J. High Energy Phys. 11 (2018) 046.

[8] Biagio Di Micco, Maxime Gouzevitch, Javier Mazzitelli, and Caterina Vernieri, Higgs boson potential at colliders: Status and perspectives, Rev. Phys. **5,** 100045 (2020); G. Heinrich, Collider physics at the precision frontier, Phys. Rep. **922,** 1 (2021).

[9] C. Autermann (ATLAS and CMS Collaborations), Search for supersymmetry at the LHC, EPJ Web Conf. **164,** 01028 (2017); A. Canepa, Searches for supersymmetry at the large hadron collider, Rev. Phys. **4,** 100033 (2019).

[10] J. Hewett and M. Spiropulu, Particle physics probes of extra spacetime dimensions, Annu. Rev. Nucl. Part. Sci. **52,** 397 (2002); T. Appelquist, H. C. Cheng, and B. A. Dobrescu, Bounds on universal extra dimensions, Phys. Rev. D **64,** 035002 (2001); H.-C. Cheng, Introduction to extra dimensions, in *Physics of the Large and the Small, TASI 09, Proceedings of the Theoretical Advanced Study Institute in Elementary Particle Physics, Boulder, Colorado, USA, 2011* (World Scientific, 2011); N. Deutschmann, T. Flacke, and J. S. Kim, Current LHC constraints on minimal universal extra dimensions, Phys. Lett. B **771,** 515 (2017); CMS Collaboration, Search for resonant and nonresonant new phenomena in high-mass dilepton final states at $\sqrt{s} = 13$ TeV, J. High Energy Phys. 07 (2021) 208; Search for large extra dimensions in the diphoton final state at the large hadron collider, J. High Energy Phys. 05 (2011) 085; Search for new physics with dijet angular distributions in proton-proton collisions at $\sqrt{s} = 13$ TeV, J. High Energy Phys. 07 (2017) 013.

[11] Y. Achiman and B. Stech, Quark-lepton symmetry and mass scales in an E6 unified gauge model, Phys. Lett. **77B,** 389 (1978); Q. Shafi, E_6 as a unifying gauge symmetry, Phys. Lett. **79B,** 301 (1978); F. Gürsey, P. Ramond, and P. Sikivie, A universal gauge theory model based on E_6, Phys. Lett. **60B,** 177 (1976); R. Barbieri, D. V. Nanopoulos, and A. Masiero, Hierarchical fermion masses in E_6, Phys. Lett. **104B,** 194 (1981); G. Dvali and Q. Shafi, On proton stability and the gauge hierarchy problem, Phys. Lett. B **403,** 65 (1997).

[12] L. Hall, Y. Nomura, and D. Smith, Gauge-Higgs unification in higher dimensions, Nucl. Phys. **B639,** 307 (2002); Y. Abe, Y. Goto, and Y. Kawamura, Left-right symmetry, orbifold S^1/Z_2 and radiative breaking of $U(1)_R \times U(1)_{B-L}$, Prog. Theor. Exp. Phys. **2018,** 103B01 (2018).

[13] P. M. Ferreira, B. L. Gonçalves, and F. R. Joaquim, The hidden side of scalar-triplet models with spontaneous *CP* violation, arXiv:2109.13179.

[14] P. S. Bhupal Dev, R. N. Mohapatra, W. Rodejohann, and Xun-Jie Xu, Vacuum structure of the left-right symmetric model, J. High Energy Phys. 02 (2019) 154.

[15] P. A. Zyla *et al.* (Particle Data Group), Review of particle physics, Prog. Theor. Exp. Phys. **2020,** 083C01 (2020).

[16] T. Bandyopadhyay, G. Bhattacharyya, D. Das, and A. Raychaudhuri, Reappraisal of constraints on Z' models from unitarity and direct searches at the LHC, Phys. Rev. D **98,** 035027 (2018).

[17] ATLAS Collaboration, Search for a right-handed gauge boson decaying into a high-momentum heavy neutrino and a charged lepton in pp collisions with the ATLAS detector at $\sqrt{s} = 13$ TeV, Phys. Lett. B **798,** 134942 (2019).

[18] F. Staub, SARAH4: A tool for (not only SUSY) model builders, Comput. Phys. Commun. **185,** 1773 (2014).

[19] A. Alloul, N. D. Christensen, C. Degrande, C. Duhr, and B. Fuks, FEYNRULES2.0—A complete toolbox for tree-level phenomenology, Comput. Phys. Commun. **185,** 2250 (2014).

[20] J. Alwall, R. Frederix, S. Frixione, V. Hirschi, F. Maltoni, O. Mattelaer, H.-S. Shao, T. Stelzer, P. Torrielli, and M. Zaro, The automated computation of tree-level and next-to-leading order differential cross sections, and their matching to parton shower simulations, J. High Energy Phys. 07 (2014) 079.

[21] R. D. Ball *et al.*, Parton distributions with LHC data, Nucl. Phys. **B867,** 244 (2013).

[22] ATLAS Collaboration, Search for new high-mass phenomena in the dilepton final state using 36.1 fb^{-1} of proton-proton collision data at $\sqrt{s} = 13$ TeV with the ATLAS detector, J. High Energy Phys. 10 (2017) 182.

[23] S. F. King, Neutrino mass models, Rep. Prog. Phys. **67,** 107 (2004); A. de Gouvêa, Neutrino mass models, Annu. Rev. Nucl. Part. Sci. **66,** 197 (2016).

[24] B. Stech and Z. Tavartkiladze, Fermion masses and coupling unification in E_6. Life in the desert, Phys. Rev. D **70,** 035002 (2004); H. Akcay, The fermion masses in E_6, Mod. Phys. Lett. A **13,** 685 (1998).

[25] T. Bandyopadhyay and R. Maji, The E_6 route to multi-component dark matter, arXiv:1911.13298.

[26] CMS Collaboration, Searches for long-lived charged particles in pp collisions at $\sqrt{s} = 7$ and 8 TeV, J. High Energy Phys. 07 (2013) 122.

[27] ATLAS Collaboration, Search for heavy charged long-lived particles in the ATLAS detector in 36.1 fb^{-1} of proton-proton collision data at $\sqrt{s} = 13$ TeV, Phys. Rev. D **99,** 092007 (2019).

[28] ATLAS Collaboration, Search for heavy neutral Higgs bosons produced in association with b-quarks and decaying to b-quarks at $\sqrt{s} = 13$ TeV with the ATLAS detector, Phys. Rev. D **102,** 032004 (2020).

[29] CMS Collaboration, Search for beyond the standard model Higgs bosons decaying into a $b\bar{b}$ pair in pp collisions at $\sqrt{s} = 13$ TeV, J. High Energy Phys. 08 (2018) 113.

[30] S. Dawson, C. B. Jackson, L. Reina, and D. Wackeroth, Higgs production in association with bottom quarks at hadron colliders, Mod. Phys. Lett. A **21,** 89 (2006).

[31] A. V. Bednyakov, B. A. Kniehl, A. F. Pikelner, and O. L. Veretin, On the b-quark running mass in QCD and the SM, Nucl. Phys. **B916,** 463 (2017).

[32] S. Dawson and R. Kauffman, QCD corrections to Higgs boson production: Nonleading terms in the heavy quark limit, Phys. Rev. D **49,** 2298 (1994); D. Graudenz, M. Spira, and P. M. Zerwas, QCD Corrections to Higgs-Boson Production at Proton-Proton Colliders, Phys. Rev. Lett. **70,** 1372 (1993).

[33] ATLAS Collaboration, Search for charged Higgs bosons decaying into a top quark and a bottom quark at $\sqrt{s} = 13$ TeV with the ATLAS detector, J. High Energy Phys. 06 (2021) 145.

[34] ATLAS Collaboration, Search for charged Higgs bosons decaying into top and bottom quarks at $\sqrt{s} = 13$ TeV with the ATLAS detector, J. High Energy Phys. 11 (2018) 085.

[35] CMS Collaboration, Search for charged Higgs bosons decaying into a top and a bottom quark in the all-jet final state of pp collisions at $\sqrt{s} = 13$ TeV, J. High Energy Phys. 07 (2020) 126.

[36] C. Degrande, Maria Ubiali, Marius Wiesemann, and Marco Zaro, Heavy charged Higgs boson production at the LHC, J. High Energy Phys. 10 (2015) 145; C. Degrande R. Frederix, V. Hirschi, M. Ubiali, M. Wiesemann, and M. Zaro, Accurate predictions for charged Higgs production: Closing the $m_H^{\pm} \sim m_t$ window, Phys. Lett. B **772,** 87 (2017).

[37] J. Alimena *et al.*, Searching for long-lived particles beyond the Standard Model at the Large Hadron Collider, J. Phys. G **47,** 090501 (2020).

[38] S. Bhattacharyya (to be published).

[39] S. Bhattacharyya (to be published).